AAC Journals.ASM.org

A New Nonpolar *N*-Hydroxy Imidazoline Lead Compound with Improved Activity in a Murine Model of Late-Stage *Trypanosoma brucei brucei* Infection Is Not Cross-Resistant with Diamidines

Carlos H. Ríos Martínez,[a] Florence Miller,[b,c*] Kayathiri Ganeshamoorthy,[d,e] Fabienne Glacial,[d,e] Marcel Kaiser,[f,g] Harry P. de Koning,[h] Anthonius A. Eze,[h*] Laura Lagartera,[a] Tomás Herraiz,[i] Christophe Dardonville[a]

Instituto de Química Médica, IQM-CSIC, Madrid, Spain[a]; Institut Necker-Enfants Malades, INSERM U1151, CNRS 8253, Paris, France[b]; Université Paris Descartes UMR_S 1151, Sorbonne Paris Cité, Paris, France[c]; Institut Cochin, Université Paris Descartes, CNRS (UMR 8104), Paris, France[d]; INSERM, U1016, Paris, France[e]; Swiss Tropical and Public Health Institute, Basel, Switzerland[f]; University of Basel, Basel, Switzerland[g]; Institute of Infection, Immunity and Inflammation, College of Medical, Veterinary and Life Sciences, University of Glasgow, Glasgow, United Kingdom[h]; Instituto de Ciencia y Tecnología de Alimentos y Nutrición, ICTAN-CSIC, Madrid, Spain[i]

Treatment of late-stage sleeping sickness requires drugs that can cross the blood-brain barrier (BBB) to reach the parasites located in the brain. We report here the synthesis and evaluation of four new *N*-hydroxy and 12 new *N*-alkoxy derivatives of bisimidazoline leads as potential agents for the treatment of late-stage sleeping sickness. These compounds, which have reduced basicity compared to the parent leads (i.e., are less ionized at physiological pH), were evaluated *in vitro* against *Trypanosoma brucei rhodesiense* and *in vivo* in murine models of first- and second-stage sleeping sickness. Resistance profile, physicochemical parameters, *in vitro* BBB permeability, and microsomal stability also were determined. The *N*-hydroxy imidazoline analogues were the most effective *in vivo*, with 4-((1-hydroxy-4,5-dihydro-1*H*-imidazol-2-yl)amino)-*N*-(4-((1-hydroxy-4,5-dihydro-1*H*-imidazol-2-yl)amino)phenyl)benzamide (14d) showing 100% cures in the first-stage disease, while 15d, 16d, and 17d appeared to slightly improve survival. In addition, 14d showed weak activity in the chronic model of central nervous system infection in mice. No evidence of reduction of this compound with hepatic microsomes and mitochondria was found *in vitro*, suggesting that *N*-hydroxy imidazolines are metabolically stable and have intrinsic activity against *T. brucei*. In contrast to its unsubstituted parent compound, the uptake of 14d in *T. brucei* was independent of known drug transporters (i.e., *T. brucei* AT1/P2 and HAPT), indicating a lower predisposition to cross-resistance with other diamidines and arsenical drugs. Hence, the *N*-hydroxy bisimidazolines (14d in particular) represent a new class of promising antitrypanosomal agents.

African trypanosomes (*Trypanosoma brucei* spp.) are protozoan parasites that cause human African trypanosomiasis (HAT, or sleeping sickness) and the corresponding animal disease (called nagana) in cattle. Despite the great harm it causes at human and socioeconomical levels in sub-Saharan Africa, sleeping sickness is still one of the most neglected tropical diseases (1). This is evidenced by the lack of acceptable treatment options for the central nervous system (CNS) stage of *T. b. rhodesiense* infection, which still relies solely on the highly toxic arsenical drug melarsoprol (2). Indeed, the only available drug for the treatment of early-stage *T. b. rhodesiense* sleeping sickness, suramin, was introduced in the early 1920s and also exhibits unacceptable side effects. Thus, new drugs that are safe and effective for early (hemolymphatic) and late (CNS) stages of HAT are needed.

Several antiparasitic dicationic drugs have been in clinical use for decades (3, 4). For example, pentamidine remains the standard drug to treat early-stage *T. b. gambiense* infection, whereas diminazene aceturate is used for animal trypanosomiasis. In recent years, the diamidine pafuramidine reached phase III clinical trials as an oral treatment for HAT. However, its development was stopped recently due to unexpected renal toxicity discovered in an extended phase I safety trial (5). Nevertheless, other CNS-permeable diamidines, such as DB829, still are being studied as possible clinical candidates for second-stage *T. b. gambiense* disease (5).

In recent years, our group has been involved in the study of diphenyl dicationic antitrypanosomal agents that hold 2-aminoimidazolinium moieties (6, 7). This class of molecules has produced very active compounds in mouse models of stage 1 trypanosome infection; some compounds were curative in a mouse model of acute HAT (*T. b. rhodesiense* STIB900) but were devoid of activity in a mouse model of CNS-stage infection, probably owing to poor brain permeation (6). Low blood-brain barrier (BBB) permeability was confirmed *in vitro* with a humanized model of brain endothelial cells (i.e., the human cerebral microvessel endothelial cell line hCMEC/D3) (8). Due to their dicationic nature, these compounds diffuse poorly across the BBB. To reduce the ioniza-

Received 27 August 2014 **Returned for modification** 13 October 2014
Accepted 13 November 2014

Accepted manuscript posted online 24 November 2014

Citation Ríos Martínez CH, Miller F, Ganeshamoorthy K, Glacial F, Kaiser M, de Koning HP, Eze AA, Lagartera L, Herraiz T, Dardonville C. 2015. A new nonpolar *N*-hydroxy imidazoline lead compound with improved activity in a murine model of late-stage *Trypanosoma brucei brucei* infection is not cross-resistant with diamidines. Antimicrob Agents Chemother 59:890–904. doi:10.1128/AAC.03958-14.

Address correspondence to Christophe Dardonville, dardonville@iqm.csic.es.

* Present address: Florence Miller, Institut de Radioprotection et de Sûreté Nucléaire (IRSN), PRP-HOM, SRBE, LRTOX, Fontenay-aux-Roses, France; Anthonius A. Eze, Department of Medical Biochemistry, University of Nigeria, Enugu Campus, Enugu, Nigeria.

Supplemental material for this article may be found at http://dx.doi.org/10.1128/AAC.03958-14.

This article is dedicated to José Elguero on the occasion of his 80th birthday.

doi:10.1128/AAC.03958-14

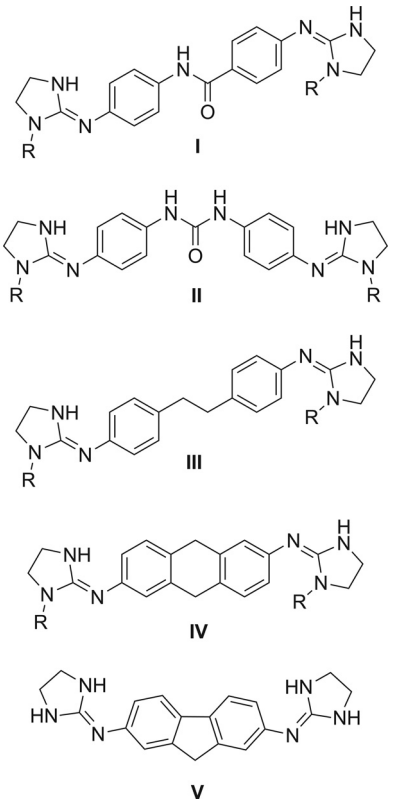

FIG 1 Lead compounds (R = H, dihydrochloride salts) with *in vivo* antitrypanosomal activity in the acute *T. b. rhodesiense* mouse model (9) and new *N*-alkoxy and *N*-hydroxy analogues (R = OMe, OEt, OTHP, OH, and OBn).

tion state of the compounds at physiological pH, a strategy consisting of derivatizing the basic nitrogens of the imidazoline ring with O-alkyl or OH substituents was tested and showed that, in this series, the *N*-hydroxy derivative had enhanced BBB permeability (8). However, this compound was only moderately active in a mouse model of first-stage HAT and was not studied further as a trypanocide.

In the current work, we have broadened the scope of our study to recently discovered bisaminoimidazoline leads (9) that are even more effective antitrypanosomal agents in an acute mouse model of infection (Fig. 1). We previously reported that these compounds (I to V) cured *T. b. rhodesiense*-infected mice by intraperitoneal administration at 20 mg/kg of body weight intraperitoneally (i.p.) (9). An *in vivo* follow-up study (see Table 3) showed that this activity was retained at low dosage (5 to 10 mg/kg i.p.) and by oral administration for I and V (50 mg/kg per os [p.o.]). However, compound I was not active and V was only weakly active in the GVR35 mouse model of late-stage disease (see Table 4), indicating that the compounds needed further optimization to attain curative concentrations in the brain.

Here, a series of nonpolar *N*-hydroxy and *N*-alkoxy derivatives of these new leads was synthesized to incorporate one OR group (R = H, Me, Et, Bn) on the N1-nitrogen of each imidazoline ring (compounds 14a to 17e) (Fig. 1). Our intention was to reduce the ionization constants (pK_a) of these leads to decrease the proportion of the ionized form of the compounds in biological fluids. The *in vitro* antiprotozoal activities of the compounds, as well as their *in vivo* antitrypanosomal effects in mouse models of stage 1 and CNS-stage HAT, were studied. In addition, the ionization constants of these derivatives were measured, important physicochemical parameters relevant to membrane permeation (e.g., calculated log of octanol-water partition coefficient [clog*P*] and log*D*) were calculated, binding to human serum albumin (HSA) was measured, and *in vitro* BBB permeability was determined using the hCMEC/D3 model. One compound, the *N*-hydroxy derivative 14d, was 100% curative in the mouse model of first-stage HAT and weakly active (i.e., increased parasite-free survival time versus that of the control) by i.p. dosage in the GVR35 chronic model, showing no overt toxicity and a higher safety profile than the corresponding parent compound I. We also investigated whether 14d was a substrate for *N*-hydroxylamine reductases occurring in hepatic fractions to give the corresponding imidazoline parent compound I, similarly to how amidoxime prodrugs generate amidine active drugs.

MATERIALS AND METHODS

Chemistry. All dry solvents were purchased from Aldrich or Fluka in Sure/Seal bottles. All reactions requiring anhydrous conditions or an inert atmosphere were performed under a positive pressure of N_2. All reactions were monitored by thin-layer chromatography (TLC) using silica gel 60 F_{254} plates (Merck) or high-performance liquid chromatography-mass spectrometry (HPLC-MS). Chromatography was performed with Isolute SI prepacked columns. ^1H and ^{13}C nuclear magnetic resonance (NMR) spectra were recorded on a Bruker Advance 300 or Varian Inova 400 spectrometer. Chemical shifts of the ^1H NMR spectra were internally referenced to the residual proton resonance of the deuterated solvents: $CDCl_3$ (7.26 ppm), D_2O (δ 4.6 ppm), CD_3OD (3.49 ppm), and dimethylsulfoxide (DMSO-d_6) (δ 2.49 ppm). *J* values are given in Hz. Signal-splitting patterns are described as singlet (s), broad singlet (br s), doublet (d), triplet (t), quadruplet (q), multiplet (m), or combinations thereof. Melting points (mp) were determined in open capillary tubes with an SMP3-Stuart Scientific apparatus or Mettler Toledo MP70 melting point system and are uncorrected. Elemental analysis was performed on a Heraeus CHN-O rapid analyzer. Analytical results were within ±0.4% of the theoretical values unless otherwise noted. Analytical HPLC-MS was run with an Xbridge C_{18}, 3.5-μm (2.1- by 100-mm) column on a Waters 2695 separation module coupled with a Waters Micromass ZQ spectrometer using electrospray ionization (ESI^+). The following HPLC conditions were used: column temperature, 30°C; gradient time, 5 min; H_2O-CH_3CN (10:90→90:10) (0.1% HCO_2H); flow rate, 1 ml/min; UV detection, diode array (wavelength [λ] of 190 to 400 nm). Accurate masses were measured with an Agilent Technologies quantitative time-of-flight 6520 spectrometer using electrospray ionization. Diamines 1 and 3 (starting material) were commercially available. Diamine 2 was obtained by reduction of the commercially available 1,3-bis(4-nitrophenyl)urea as described previously (9).

Diamine 4. 9,10-Dihydroanthracene-2,6-diamine (diamine 4) was synthesized using a modification of the procedure described by Takimiya et al. (10). A Kimax tube was charged with 2,6-diamino-9,10-anthraquinone (1.08 g; 4.5 mmol), activated zinc (4.5 g; 68 mmol), and 30% aqueous ammonia (10 ml). (For the activation of zinc, zinc powder was stirred with 10% aqueous HCl solution for 2 min, collected on a fritted filter, and rinsed with H_2O and acetone successively. The powder was transferred to a flask and vigorously shaken with diethyl ether (Et_2O) for 10 min. The activated zinc powder was drained, rinsed with Et_2O, and used in the reaction.) The tube was stoppered and heated at 100°C for 23 h. The green precipitate was collected by filtration on Celite. The filter cake was rinsed thoroughly with acetone (250 ml) to extract the product (yellow) out of the zinc salts. The yellow (fluorescent) acetone filtrate was dried (Na_2SO_4), and the solvent was evaporated to give diamine 4 as a yellow solid (830 mg, 88%). The product was >90% pure and used without further purification. Alternatively, the product can be recrystallized in

methanol (MeOH). ^{1}H NMR data were consistent with the reported ones (10).

Synthesis of isothiocyanates 5 to 8. Thiophosgene (2.5 equivalents [equiv]), a highly toxic reagent that must be handled with adequate protecting clothes in a well-ventilated fumehood, was added with a syringe to a stirred suspension of diamines 1 to 4 (1 equiv) in Et_2O-H_2O (3:1, vol/vol). The reaction mixture was stirred at room temperature overnight. The precipitate was filtered, rinsed with water, and dried under vacuum to yield the isothiocyanates 5 to 8 in excellent yields and of adequate purity.

(i) 4-Isothiocyanato-*N*-(4-isothiocyanatophenyl)benzamide (5). Diamine 1 (3.42 g; 15 mmol) and thiophosgene (2.51 ml; 33 mmol) were reacted according to the general protocol described above to yield compound 5 as a gray solid (92%). HPLC (UV), >95%; mp, 199 to 200°C; ^{1}H NMR (300 MHz, $CDCl_3$) δ 7.88 (br s, 1H, *NH*), 7.85 (d, *J* = 8.7, 2H, Ar*H*), 7.63 (d, *J* = 8.8, 2H, Ar*H*), 7.31 (d, *J* = 8.7, 2H, Ar*H*), 7.22 (d, *J* = 8.8, 2H, Ar*H*). ^{13}C NMR (75 MHz, $CDCl_3$) δ 164.7, 138.6, 137.1, 135.9, 135.5, 133.2, 129.0, 127.8, 127.0, 126.5, 121.5. Low-resolution mass spectrometry (LRMS) (ESI^+) *m/z* = 312.27 (M + H).

(ii) 1,3-Bis(4-isothiocyanatophenyl)urea (6). Diamine 2 (2.02 g; 8.84 mmol) and thiophosgene (1.69 ml; 22.1 mmol) were reacted according to the general protocol to yield 6 as a gray solid (78%). HPLC (UV), >95%; mp, >235°C; ^{1}H NMR (300 MHz, $CDCl_3$) δ 8.29 (br s, 2H, *NH*), 7.40 (d, *J* = 8.8, 4H, Ar*H*), 7.12 (d, *J* = 8.8, 4H, Ar*H*). LRMS (ES^+) *m/z* = 327.19 (M+H).

(iii) 1,2-Bis(4-isothiocyanatophenyl)ethane (7). Diamine 3 (3.23 g; 15.2 mmol) and thiophosgene (2.55 ml; 33.5 mmol) were reacted according to the general protocol to yield 7 as an off-white solid (84%). HPLC (UV), 95%; mp, 128 to 129°C. ^{1}H NMR (300 MHz, $CDCl_3$) δ 7.13 (m, 4H, Ar*H*), 7.06 (m, 4H, Ar*H*), 2.89 (s, 4H, CH_2).

(iv) 2,6-Diisothiocyanato-9,10-dihydroanthracene (8). Diamine 4 (2.46 g; 11.7 mmol) and thiophosgene (1.96 ml; 26 mmol) were reacted according to the general protocol to yield 8 as a beige solid (89%). HPLC (UV), >90%; mp, >300°C. ^{1}H NMR (300 MHz, DMSO) δ 7.42 (d, *J* = 1.9, 2H, Ar*H*), 7.40 (d, *J* = 8.0, 2H, Ar*H*), 7.27 (dd, *J* = 1.9, 8.0, 2H, Ar*H*), 3.94 (s, 4H, CH_2). ^{13}C NMR (75 MHz, $CDCl_3$) δ 137.9, 136.0, 132.9, 128.5, 127.7, 124.5, 123.6, 34.4.

General procedure for the synthesis of 1-alkoxy-2-arylaminoimidazolines 14a, 14b, 15b, 15e, 16a, and 17a. A suspension of isothiocyanate (compounds 5 to 8; 1 equiv) in dry dimethylformamide (DMF) (5 ml) was added dropwise to a stirred solution of compounds 9a to 9d (2.5 equiv) in dry DMF (5 ml) under an argon atmosphere. The flask containing the isothiocyanate suspension was rinsed with approximately 20 ml of dry DMF that subsequently was added to the reaction mixture. The reaction mixture was stirred at room temperature, and the formation of the intermediate thiourea (compounds 10 to 13) was checked by HPLC-MS. Nosyl group removal was performed in the same flask by addition of thiophenol (10 equiv) and K_2CO_3 (20 equiv). The reaction mixture was warmed to 65°C and stirred until complete cyclization to the final 1-alkoxy-2-arylaminoimidazolines 14a, 14b, 15b, 15e, 16a, and 17a. The crude reaction mixture was filtered on Celite, and the filter cake was rinsed with CH_2Cl_2. The organic phase was washed successively with saturated $NaHCO_3$ solution (30 ml) and brine (30 ml) and dried over $MgSO_4$. The solvents were removed under vacuum, and the crude residue was purified by silica chromatography.

(i) 4-((1-Methoxy-4,5-dihydro-1*H*-imidazol-2-yl)amino)-*N*-(4-((1-methoxy-4,5-dihydro-1*H*-imidazol-2-yl)amino)phenyl)benzamide (14a). The reaction was carried out by following the general procedure described above with compounds 5 (420 mg; 1.32 mmol) and 9a (900 mg; 3.3 mmol). Purification by silica chromatography (10-g prepacked cartridge) eluting with CH_2Cl_2-MeOH (9:1) with 0.1% of triethylamine (Et_3N) yielded 14a as a brown solid (420 mg, 75%). HPLC (UV), >91%; mp, 165 to 170°C. ^{1}H NMR (300 MHz, $CDCl_3$) δ 8.41 (br s, 1H, CO*NH*), 7.68 (d, *J* = 8.5, 2H, Ar*H*), 7.41 (d, *J* = 8.5, 2H, Ar*H*), 7.27 (d, *J* = 8.5, 2H, Ar*H*), 7.16 (d, *J* = 8.5, 2H, Ar*H*), 6.13 to 5.25 (br s, 2H, *NH*), 3.70 (s, 6H, OCH_3) 3.42 (m, 4H, NCH_2), 3.33 (m, 4H, NCH_2). ^{13}C NMR (75 MHz, $CDCl_3$) δ 165.8, 158.5, 158.0, 138.9, 133.3, 128.6 (2×C), 128.4, 121.8 (2×C), 120.4 (2×C), 119.5 (2×C), 115.5, 63.1 (2×C), 51.8 (2×C), 45.8 (2×C). LRMS (ESI^+) *m/z* = 424.23 (M + H). High-resolution mass spectrometry (HRMS) (ESI^+) $C_{21}H_{25}N_7O_3$ requires 423.2019 (found: 423.2023).

(ii) 4-((1-Ethoxy-4,5-dihydro-1*H*-imidazol-2-yl)amino)-*N*-(4-((1-ethoxy-4,5-dihydro-1*H*-imidazol-2-yl)amino)phenyl)benzamide (14b). The reaction was carried out by following the general procedure with 5 (680 mg; 2.26 mmol) and 9b (1.63 g; 5.6 mmol). In this case, the cyclization process was very slow and required 24 days of stirring at 65°C. Purification by silica chromatography (20-g prepacked cartridge) eluting with CH_2Cl_2-MeOH (100:0→90:10) yielded 14b as a brown solid (50 mg; 5%). HPLC (UV), >90%; mp, 135 to 136°C. ^{1}H NMR (300 MHz, $CDCl_3$) δ 8.85 (br s, 1H, CO*NH*), 7.75 (d, *J* = 8.5, 2H, Ar*H*), 7.49 (d, *J* = 8.2, 2H, Ar*H*), 7.30 (d, *J* = 8.2, 2H, Ar*H*), 7.17 (d, *J* = 8.5, 2H, Ar*H*), 5.88 (br s, 2H, *NH*), 3.93 (q, *J* = 7.0, 4H, O$CH_2$$CH_3$), 3.53 to 3.28 (m, 8H, NCH_2), 1.24 (t, *J* = 7.0, 6H, OCH$_2$$CH_3$). ^{13}C NMR (75 MHz, $CDCl_3$) δ 165.9, 159.0, 158.4, 146.0, 138.0, 133.7, 128.6 (2×C), 128.3, 121.8 (2×C), 120.4 (2×C), 119.3 (2×C), 70.90, 70.88, 52.6 (2×C), 45.7 (2×C), 14.3 (2×C). LRMS (ESI^+) *m/z* = 452.12 (M + H). HRMS (ESI^+) $C_{23}H_{29}N_7O_3$ requires 451.2332 (found: 451.2335).

(iii) 1,3-Bis(4-((1-ethoxy-4,5-dihydro-1*H*-imidazol-2-yl)amino)phenyl)urea (15b). The reaction was carried out by following the general procedure with compounds 6 (737 mg; 2.26 mmol) and 9b (1.63 g; 5.6 mmol). In this case, the cyclization process required 11 days of stirring at 65°C. Purification by silica chromatography (20-g prepacked cartridge) eluting with CH_2Cl_2-MeOH (100:0→90:10) yielded 15b as a brown solid (253 mg; 24%). HPLC (UV), >95%; mp, 144 to 146°C. ^{1}H NMR (300 MHz, $CDCl_3$) δ 8.53 (br s, 2H, *NH*), 7.21 (d, *J* = 8.0, 4H, Ar*H*), 7.04 (d, *J* = 8.0, 4H, Ar*H*), 4.40 (br s, 2H, *NH*) 3.96 (q, *J* = 7.0, 4H, O$CH_2$$CH_3$), 3.40 (m, 8H, N$CH_2$), 1.26 (t, *J* = 7.0, 6H, OCH$_2$$CH_3$). ^{13}C NMR (75 MHz, $CDCl_3$) δ 159.5 (2×C), 154.4, 136.7 (2×C), 135.2, 128.8, 124.4, 121.4 (4×C), 120.4 (4×C), 71.1 (2×C), 52.6 (2×C), 44.8 (2×C), 14.3 (2×C). LRMS (ESI^+) *m/z* = 467.14 (M + H).

(iv) 1,3-Bis(4-((1-(benzyloxy)-4,5-dihydro-1*H*-imidazol-2-yl)amino)phenyl)urea (15e). The reaction was carried out by following the general procedure with 6 (300 mg; 0.92 mmol) and 9e (418 mg; 1.19 mmol). In this case, the cyclization process required 22 days of stirring at 65°C. Purification by silica chromatography (10-g prepacked cartridge) eluting with CH_2Cl_2-MeOH (100:0→90:10) yielded 15e as a brown solid (60 mg; 11%). HPLC (UV), 91%; mp, 60 to 65°C. ^{1}H NMR (300 MHz, $CDCl_3$) δ 8.54 (br s, 2H, *NH*), 7.44 to 7.25 (m, 10H, Ar*H*), 7.15 (d, *J* = 8.6, 4H, Ar*H*), 6.88 (d, *J* = 8.6, 4H, Ar*H*), 4.90 to 4.73 (s, 4H, OCH_2), 4.56 (br s, 2H, *NH*), 3.29 (m, 4H, NCH_2), 3.17 (m, 4H, NCH_2). ^{13}C NMR (75 MHz, $CDCl_3$) δ 159.5 (2×C), 153.9, 136.2 (2×C), 135.2 (2×C), 134.9 (2×C), 129.3 (4×C), 128.7 (2×C), 128.6 (4×C), 121.3 (4×C), 120.2 (4×C), 77.8 (2×C), 52.4 (2×C), 44.4 (2×C). LRMS (ESI^+) *m/z* = 591.49 (M + H).

(v) *N*,*N*′-(ethane-1,2-diylbis(4,1-phenylene))bis(1-methoxy-4,5-dihydro-1*H*-imidazol-2-amine) (16a). The reaction was carried out by following the general procedure with compounds 7 (420 mg; 1.32 mmol) and 9a (900 mg; 3.3 mmol). Purification by silica chromatography (10-g prepacked cartridge) eluting with CH_2Cl_2-MeOH (9:1) and 0.1% Et_3N yielded 16a as a brown solid (470 mg; 87%). HPLC (UV), >90%; mp, 106 to 108°C. ^{1}H NMR (300 MHz, $CDCl_3$) δ 8.05 (br s, 2H, *NH*), 7.32 (d, *J* = 8.2, 4H, Ar*H*), 7.10 (d, *J* = 8.2, 4H, Ar*H*), 3.82 (s, 6H, OCH_3), 3.62 (t, *J* = 6.8, 4H, NCH_2), 3.46 (t, *J* = 6.8, 4H, NCH_2), 3.10 to 2.77 (m, 4H, CH_2). ^{13}C NMR (75 MHz, $CDCl_3$) δ 158.8 (2×C), 136.3 (2×C), 129.3 (4×C), 127.2 (2×C), 119.7 (4×C), 63.2 (2×C), 52.0 (2×C), 46.8 (2×C), 37.5 (2×C). LRMS (ESI^+) *m/z* = 409.20 (M + H). HRMS (ESI^+) $C_{22}H_{28}N_6O_2$ requires 408.2274 (found: 408.2278).

(vi) N^2,N^6-bis(1-methoxy-4,5-dihydro-1*H*-imidazol-2-yl)-9,10-dihydroanthracene-2,6-diamine (17a). The reaction was carried out by following the general procedure with compounds 8 (392 mg;1.32 mmol) and 9a (900 mg; 3.3 mmol). Purification by silica chromatography

(10-g prepacked cartridge) eluting with CH_2Cl_2-MeOH (9:1) and 0.1% Et_3N yielded the product as an 8:2 mixture of 17a and 18a as a brown solid (389 mg; 72%). HPLC (UV), >90%; mp, 110 to 112°C. ^{1}H NMR (300 MHz, $CDCl_3$) δ 7.36 (s, 2H, Ar*H*), 7.12 (s, 4H, Ar*H*), 3.82 (s, 4H, CH_2), 3.78 (s, 6H, OCH_3), 3.63 to 3.51 (m, 4H, NCH_2), 3.50 to 3.34 (m, 4H, NCH_2). ^{13}C NMR (75 MHz, $CDCl_3$) δ 158.6 (2×C), 137.6 (2×C), 131.3 (2×C), 127.8 (2×C), 124.9 (2×C), 118.8 (2×C), 117.7 (2×C), 63.0 (2×C), 51.5 (2×C), 46.0 (2×C), 35.5 (2×C). LRMS (ESI^+) *m/z* = 407.11 (M + H).

General procedure for the synthesis of 1-(2-(alkoxyamino)ethyl)-3-arylthioureas 10c, 11a, 11c, 12b and 12c, and 13b and c. A suspension of isothiocyanates 5 to 8 (2.4 mmol; 1 equiv) in dry DMF (5 ml) was added dropwise to a stirred solution of compounds 9a to 9c (6 mmol; 2.5 equiv) in dry DMF (5 ml) under an argon atmosphere. The flask containing the isothiocyanate suspension was rinsed with approximately 20 ml of dry DMF that was added subsequently to the reaction mixture. The reaction mixture was stirred at room temperature for 12 h. The solvent was removed under high vacuum, and the crude product was treated with methanol. Trituration with a spatula yielded a crude solid that was filtered and washed with MeOH. The compounds were purified as specified below.

(i) 4-(3-(2-(2-Nitro-*N*-((tetrahydro-2*H*-pyran-2-yl)oxy)phenylsulfonamido)ethyl)thioureido)-*N*-(4-(3-(2-(2-nitro-*N*-((tetrahydro-2*H*-pyran-2-yl)oxy)phenylsulfonamido)ethyl)thioureido)phenyl)benzamide (10c). The reaction was carried out by following the general procedure described above with compounds 5 (750 mg; 2.4 mmol) and 9c (2.07 g; 6.0 mmol). The product was purified by precipitation from MeOH. Compound 10c was obtained as a light yellow solid (1.18 g; 41%). HPLC (UV), >95%; mp, 132 to 133°C. ^{1}H NMR (300 MHz, $CDCl_3$) δ 8.01 to 7.78 (m, 6H), 7.74 (m, 4H), 7.62 (m, 2H), 7.35 (d, *J* = 8.2, 2H), 7.21 (d, *J* = 8.2, 2H), 4.96 (d, *J* = 6.8, 1H, O*CH*), 4.88 (d, *J* = 7.2, 1H, O*CH*), 4.37 to 4.19 (m, 2H, OCH_2), 3.99 to 3.83 (m, 2H, NCH_2), 3.73 to 3.56 (m, 2H, NCH_2), 3.50 to 3.32 (m, 2H, NCH_2), 3.20 to 3.02 (m, 2H, NCH_2), 2.76 (m, 2H, OCH_2), 1.94 to 1.61 (m, 4H, CH_2), 1.56 to 1.28 (m, 8H, CH_2). ^{13}C NMR (75 MHz, $CDCl_3$) δ 180.3, 179.9, 165.2, 149.8, 149.7, 140.3, 137.2, 135.8, 135.6, 132.54, 132.51, 132.4, 132.0 (2×C), 131.5, 131.4, 129.2 (2×C), 126.2 (2×C), 125.4, 124.24, 124.21, 123.7 (2×C), 121.9, 105.9, 105.8, 65.8, 65.6, 52.8, 52.6, 41.6, 41.5, 28.9 (2×C), 24.6 (2×C), 21.2 (2×C). LRMS (ESI^+) *m/z* = 1002.45 (M + H).

(ii) 1,3-Bis(4-(3-(2-*N*-methoxy-2-nitrophenylsulfonamido)ethyl)thioureido)phenylurea (11a). The reaction was carried out by following the general procedure with compounds 6 (750 mg; 2.4 mmol) and 9a (2.07 g; 6.0 mmol). Purification by silica chromatography (10-g prepacked cartridge) eluting with hexane-ethyl acetate (EtOAc) (100:0→0:100) yielded 11a as a light green solid (774 mg; 91%). HPLC (UV), >95%; mp, >182°C (decompose). ^{1}H NMR (400 MHz, DMSO) δ 9.60 (br s, 2H, *NH*), 8.69 (br s, 2H, *NH*), 8.14 to 7.98 (m, 6H, Ar*H*), 7.97 to 7.87 (m, 2H, Ar*H*), 7.73 (br s, 2H, *NH*), 7.42 (d, *J* = 8.6, 4H, Ar*H*), 7.24 (d, *J* = 8.6, 4H, Ar*H*), 3.83 (s, 6H, OCH_3), 3.75 (m, 4H, NCH_2), 3.29 to 3.17 (m, 4H, NCH_2). ^{13}C NMR (101 MHz, DMSO) δ 180.6 (2×C), 152.5, 149.3 (2×C), 136.8 (2×C), 136.5 (2×C), 132.6, 132.0, 131.9 (2×C), 124.7 (2×C), 124.1 (4×C), 123.7 (2×C), 118.5 (2×C), 65.4 (2×C), 51.8 (4×C), 41.1 (4×C). LRMS (ESI^+) *m/z* = 877.65 (M + H).

(iii) 1,3-Bis(4-(3-(2-(*N*-tetrahydro-2*H*-pyran-2-yl)oxy-2-nitrophenylsulfonamido)ethyl)thioureido)phenylurea (11c). The reaction was carried out by following the general procedure with compounds 6 (722 mg; 2.44 mmol) and 9c (2.1 g; 6.26 mmol). Purification by silica chromatography eluting with hexane-EtOAc (100:0→0:100) yielded 11c as a light yellow solid (806 mg; 32%). HPLC (UV), >95%; mp, 164 to 166°C. ^{1}H NMR (400 MHz, DMSO) δ 9.68 (br s, 2H, *NH*), 8.70 (br s, 2H, *NH*), 8.12 to 8.00 (m, 6H, Ar*H*), 7.97 to 7.89 (m, 2H, Ar*H*), 7.43 (d, *J* = 8.8, 4H, Ar*H*), 7.31 (br s, 2H, N*H*), 7.21 (d, *J* = 8.8, 4H, Ar*H*), 5.11 to 4.75 (m, 2H, O*CH*), 4.13 to 3.93 (m, 2H, OCH_2), 3.79 to 3.62 (m, 4H, NCH_2), 3.59 to 3.46 (m, 2H, OCH_2), 3.42 to 3.35 (m, 2H, OCH_2), 2.91 to 2.75 (m, 2H, NCH_2), 1.88 to 1.60 (m, 4H, CH_2), 1.58 to 1.24 (m, 8H, CH_2). ^{13}C NMR (101 MHz, DMSO) δ 180.3 (2×C), 152.5, 148.9 (2×C), 137.0 (2×C), 136.6 (2×C), 132.2 (2×C), 124.9 (2×C), 124.2 (4×C), 123.9 (2×C), 118.7 (4×C), 104.9 (2×C), 64.0 (2×C), 52.0 (4×C), 40.6 (4×C), 28.3 (2×C), 24.3 (2×C), 19.7 (2×C). LRMS (ESI^+) *m/z* = 1,017.91 (M + H).

(iv) *N*,*N*′-(((((ethane-1,2-diylbis(4,1-phenylene))bis(azanediyl))bis(carbonothioyl))bis(azanediyl))bis(ethane-2,1-diyl))bis(*N*-ethoxy-2-nitrobenzenesulfonamide) (12b). The reaction was carried out by following the general procedure with compounds 7 (740 mg; 2.5 mmol) and 9b (1.81 g; 6.23 mmol). The product was purified by precipitation from MeOH as a light yellow solid (1.98 g; 91%). HPLC (UV), 95%; mp, 198 to 200°C. ^{1}H NMR (400 MHz, DMSO) δ 9.66 (br s, 2H, *NH*), 8.05 (m, 6H, Ar*H*), 7.97 to 7.89 (m, 2H, Ar*H*), 7.80 (br s, 2H, *NH*), 7.29 (d, *J* = 8.5, 4H, Ar*H*), 7.22 (d, *J* = 8.5, 4H, Ar*H*), 4.09 (q, *J* = 7.0, 4H, OCH_2CH$_3$), 3.75 (m, 4H, NCH_2), 3.25 (m, 4H, NCH_2), 2.84 (s, 4H, PhCH_2), 1.18 (t, *J* = 7.0, 6H, OCH$_2$$CH_3$). ^{13}C NMR (101 MHz, DMSO) δ 180.5 (2×C), 149.2 (2×C), 137.8 (2×C), 136.7 (2×C), 136.4 (2×C), 132.0 (2×C), 132,0 (2×C), 128.6 (4×C), 124.1 (2×C), 123.7 (2×C), 123.3 (4×C), 73.4 (2×C), 51.8 (2×C), 41,0 (2×C), 36.5 (2×C), 13.3 (2×C). LRMS (ESI^+) *m/z* = 875.69 (M + H).

(v) *N*,*N*′-(((((ethane-1,2-diylbis(4,1-phenylene))bis(azanediyl))bis(carbonothioyl))bis(azanediyl))bis(ethane-2,1-diyl))bis(2-nitro-*N*-((tetrahydro-2*H*-pyran-2-yl)oxy)benzenesulfonamide) (12c). The reaction was carried out by following the general procedure with 7 (722 mg; 2.44 mmol) and 9c (2.1 g; 6.26 mmol). The product was purified by precipitation from cold CH_2Cl_2. Recrystallization in cold CH_2Cl_2 yielded 12c as a white solid (1.25 g; 52%). HPLC (UV), 92%; mp, 104 to 105°C. ^{1}H NMR (400 MHz, DMSO) δ 9.76 (br s, 2H, *NH*), 8.13 to 8.00 (m, 6H, Ar*H*), 7.98 to 7.90 (m, 2H, Ar*H*), 7.39 (br s, 2H, *NH*), 7.25 (s, 8H, Ar*H*), 5.01 to 4.97 (m, 2H, O*CH*), 4.08 to 3.98 (m, 2H, OCH_2), 3.76 to 3.65 (m, 4H, NCH_2), 3.58 to 3.49 (m, 2H, NCH_2), 3.34 to 3.30 (m, 2H, NCH_2), 2.84 (s, 4H, PhCH_2), 2.83 to 2.76 (m, 2H), 1.88 to 1.77 (m, 2H), 1.67 (s, 2H), 1.56 to 1.34 (m, 8H). ^{13}C NMR (101 MHz, DMSO) δ 180.2 (2×C), 149.0 (2×C), 138.3 (2×C), 136.6 (2×C), 136.3 (2×C), 132.2 (2×C), 128.9 (2×C), 124.3 (2×C), 123.9 (2×C), 123.8, 104.9 (2×C), 64.0 (2×C), 52.0 (2×C), 40.6 (2×C), 36.6 (2×C), 28.3 (2×C), 24.3 (2×C), 19.7 (2×C). LRMS (ESI^+) *m/z* = 988 (M + H).

(vi) *N*,*N*′-(((((9,10-dihydroanthracene-2,6-diyl)bis(azanediyl))bis(carbonothioyl))bis(azanediyl))bis(ethane-2,1-diyl))bis(*N*-ethoxy-2-nitrobenzenesulfonamide) (13b). The reaction was carried out by following the general procedure with 8 (0.61 g; 2.08 mmol) and 9b (1.49 g; 5.2 mmol). The product was purified by silica chromatography with hexane-EtOAc (80:20→0:100) and yielded 13b as a light brown solid (562 mg; 32%). HPLC (UV), 95%; mp, 126 to 127°C. ^{1}H NMR (400 MHz, DMSO) δ 9.67 (br s, 2H), 8.16 to 7.98 (m, 6H), 7.98 to 7.90 (m, 2H), 7.77 (br s, 2H), 7.33 (m, 2H), 7.27 (d, *J* = 8.0, 2H), 7.14 (d, *J* = 8.0, 2H), 4.11 (q, *J* = 7.1, 4H), 3.87 (s, 4H), 3.79 to 3.67 (m, 4H), 3.30 to 3.17 (m, 4H), 1.18 (t, *J* = 7.1, 6H). ^{13}C NMR (101 MHz, DMSO) δ 180.6 (2×C), 149.2 (2×C), 137.2, 136.7, 136.4 (2×C), 132.9, 132.25, 132.19, 127.5 (2×C), 124.1 (2×C), 123.8 (2×C), 122.5 (2×C), 121.5 (2×C), 73.4 (2×C), 51.8 (2×C), 41.0 (2×C), 35.0 (2×C), 13.3 (2×C). (ESI^+) *m/z* = 873.7 (M + H).

(vii) *N*,*N*′-(((((9,10-dihydroanthracene-2,6-diyl)bis(azanediyl))bis(carbonothioyl))bis(azanediyl))bis(ethane-2,1-diyl))bis(2-nitro-*N*-((tetrahydro-2*H*-pyran-2-yl)oxy)benzenesulfonamide) (13c). The reaction was carried out by following the general procedure with compounds 8 (0.722 g; 2.44 mmol) and 9c (2.1 g; 6.26 mmol). Purification by silica chromatography with hexane-EtOAc (100:0→0:100) yielded 13c as a brown solid (846 mg; 35%). HPLC (UV), >90%; mp, 116 to 118°C. ^{1}H NMR (400 MHz, DMSO) δ 9.79 (br s, 2H), 8.14 to 8.01 (m, 6H), 7.99 to 7.91 (m, 2H), 7.37 to 7.25 (m, 4H), 7.17 to 7.05 (m, 2H), 4.92 to 4.88 (m, 2H), 4.14 to 4.06 (m, 2H), 3.89 (s, 4H), 3.80 to 3.64 (m, 2H), 3.61 to 3.44 (m, 4H), 3.14 to 3.06 (m, 2H), 2.81 (m, 2H), 1.76 (m, 2H), 1.61 (m, 2H), 1.32 (m, 8H). ^{13}C NMR (101 MHz, DMSO) δ 180.2 (2×C), 149.8 (2×C), 137.5, 136.6, 136.2, 133.6, 132.25, 132.19, 127.7 (2×C), 124.2 (2×C), 123.8 (2×C), 122.9 (2×C), 122.0 (2×C), 104.9 (2×C), 64.0 (2×C), 52.0

(2×C), 40.5 (2×C), 35.0 (2×C), 28.3, 24.2 (2×C), 19.7 (2×C), 14.1 (2×C). LRMS (ESI^+) m/z = 985.75 (M + H).

General procedure for the synthesis of 1-alkoxy-2-arylaminoimidazolines 14c, 15a, 15c, 16b, 16c, 17b, and 17c from the corresponding thioureas. Thiophenol (6 equiv) and K_2CO_3 (12 equiv) were added to a stirred solution of thiourea in dry DMF (100 ml). After the removal of the nosyl-protecting groups (checked by HPLC-MS), the reaction mixture was diluted with dry DMF (100 ml). The reaction mixture was stirred for several days at room temperature (times are indicated for each compound) until the formation of the final products (checked by HPLC-MS). Solvents were removed under vacuum, and the crude residue was dissolved in CH_2Cl_2. The precipitate was filtered off, and the filtrate was washed with 5% aqueous $NaHCO_3$ solution (1 × 50 ml) and brine (1 × 50 ml). The organic phase was dried ($MgSO_4$) and evaporated to yield crude 1-alkoxy-2-arylaminoimidazoline. Compounds were purified by silica chromatography (10-g prepacked cartridge) using CH_2Cl_2-MeOH (100:0→90:10) (14c, 15c, 16c, and 17c) or CH_2Cl_2-NH_3-saturated MeOH (100:0→90:10) (15d). Compounds 15a and 16b were purified by neutral alumina chromatography using CH_2Cl_2-NH_3-saturated MeOH (100:0→90:10).

(i) *N*-(4-((1-hydroxy-4,5-dihydro-1*H*-imidazol-2-yl)amino)phenyl)-4-((1-((tetrahydro-2*H*-pyran-2-yl)oxy)-4,5-dihydro-1*H*-imidazol-2-yl)amino)benzamide (14c). The reaction was carried out by following the general procedure described above with compound 10c (570 mg; 0.57 mmol), thiophenol (0.349 ml, 3.41 mmol), and K_2CO_3 (943 mg; 6.38 mmol) at room temperature for 5 days. Purification by silica chromatography as described above yielded 14c as a brown solid (147 mg; 46%). HPLC (UV), 95%; mp, 121 to 123°C. ^{1}H NMR (300 MHz, $CDCl_3$) δ 8.03 (br s, 1H, CO*NH*), 7.80 (d, J = 8.7, 2H, Ar*H*), 7.57 (dd, J = 2.4, 8.7, 4H, Ar*H*), 7.42 (d, J = 8.7, 2H, Ar*H*), 4.95 to 4.80 (m, 2H, O*CH*), 4.21 to 4.07 (m, 2H, OCH_2), 3.71 to 3.54 (m, 8H, NCH_2), 3.39 to 3.25 (m, 2H, OCH_2), 2.01 to 1.73 (m, 4H, CH_2), 1.69 to 1.64 (m, 8H, CH_2). ^{13}C NMR (75 MHz, $CDCl_3$) δ 165.4, 159.6, 159.1, 143.8, 136.5, 133.1, 128.3 (2×C), 127.9, 121.3 (2×C), 119.2 (2×C), 117.7 (2×C), 105.1, 104.9, 66.4, 66.0, 53.8 (2×C), 49.8, 48.9, 29.4, 29.4, 25.0 (2×C), 21.7, 21.5. LRMS (ESI^+) m/z = 564.47 (M + H).

(ii) 1,3-Bis(4-((1-methoxy-4,5-dihydro-1*H*-imidazol-2-yl)amino)phenyl)urea (15a). The reaction was carried out by following the general procedure with compound 11a (1,59 g; 1.8 mmol), thiophenol (0.49 ml, 4.8 mmol), and K_2CO_3 (1.32 g; 9.6 mmol) at room temperature for 7 days. Purification by alumina chromatography as described above yielded 15a as a brown solid (83 mg; 10%). HPLC (UV), 97%; mp, >135°C (decompose). ^{1}H NMR (400 MHz, DMSO) δ 9.54 (br s, 2H, *NH*), 7.45 (d, J = 8.8, 4H, Ar*H*), 7.37 (d, J = 8.8, 4H, Ar*H*), 3.77 (s, 6H, OCH_3), 3.58 (t, J = 7.1, 4H, NCH_2), 3.48 (t, J = 7.1, 4H, NCH_2). ^{13}C NMR (101 MHz, DMSO) δ 159.0, 152.8 (2×C), 136.7 (2×C), 132.1 (2×C), 122.6 (4×C), 118.4 (4×C), 63.1 (2×C), 50.6 (2×C), 43.5 (2×C). LRMS (ES^+) m/z = 439.45 (M + H).

(iii) 1,3-Bis(4-((1-((tetrahydro-2*H*-pyran-2-yl)oxy)-4,5-dihydro-1*H*-imidazol-2-yl)amino)phenyl)urea (15c). The reaction was carried out by following the general procedure with 11c (570 mg; 0.8 mmol), thiophenol (0.348 ml, 3.41 mmol), and K_2CO_3 (943 mg; 6.83 mmol) at room temperature for 5 days. Purification by silica chromatography as described above yielded 15c as a brown solid (53 mg; 11%). HPLC (UV), >90%; mp, 108 to 110°C. ^{1}H NMR (300 MHz, $CDCl_3$) δ 7.87 (br s, 2H, *NH*), 7.26 to 7.14 (m, 8H, Ar*H*), 4.88 (d, J = 5.0, 2H, O*CH*), 4.19 to 3.98 (m, 2H, OCH_2), 3.66 to 3.46 (m, 8H, NCH_2), 3.45 to 3.19 (m, 2H, OCH_2), 2.07 to 1.71 (m, 4H, CH_2), 1.70 to 1.38 (m, 8H, CH_2). ^{13}C NMR (75 MHz, $CDCl_3$) δ 159.8 (2×C), 153.9, 135.9 (2×C), 134.0 (2×C), 120.7 (4×C), 120.0 (4×C), 104.5 (2×C), 65.5 (2×C), 53.7 (2×C), 48.1 (2×C), 29.1 (2×C), 24.9 (2×C), 21.8 (2×C). LRMS (ESI^+) m/z = 579.52 (M + H).

(iv) *N*,*N*′-(ethane-1,2-diylbis(4,1-phenylene))bis(1-ethoxy-4,5-dihydro-1*H*-imidazol-2-amine) (16b). The reaction was carried out by following the general procedure with 12b (900 mg; 1.1 mmol), thiophenol (0.68 ml, 6.6 mmol), and K_2CO_3 (1.82 g; 13.2 mmol) at room temperature for 7 days. Purification by alumina chromatography as described above yielded 16b as a brown solid (45 mg; 5.6%). HPLC (UV), 97%; mp, 65 to 70°C. ^{1}H NMR (400 MHz, $CDCl_3$) δ 7.28 (d, J = 8.4, 4H, Ar*H*), 7.05 (d, J = 8.4, 4H, Ar*H*), 5.28 (br s, 2H, *NH*), 3.98 (q, J = 7.0, 4H, OCH_2CH$_3$), 3.57 (t, J = 7.2, 4H, NCH_2), 3.39 (t, J = 7.2, 4H, NCH_2), 2.81 (s, 4H, PhCH_2), 1.31 (t, J = 7.0, 6H, OCH$_2$$CH_3$). ^{13}C NMR (101 MHz, $CDCl_3$) δ 159.1 (2×C), 138.4 (2×C), 136.1 (2×C), 129.1 (4×C), 127.1 (4×C), 119.4 (2×C), 70.9 (2×C), 53.0 (2×C), 47.2 (2×C), 37.4 (2×C), 14.4 (2×C). LRMS (ESI^+) m/z = 437.49 (M + H).

(v) *N*,*N*′-(ethane-1,2-diylbis(4,1-phenylene))bis(1-((tetrahydro-2*H*-pyran-2-yl)oxy)-4,5-dihydro-1*H*-imidazol-2-amine) (16c). The reaction was carried out by following the general procedure with 12c (448 mg; 0.45 mmol), thiophenol (0.275 ml, 2.7 mmol), and K_2CO_3 (745 mg; 5.4 mmol) at room temperature for 13 days. Purification by silica chromatography as described above yielded 16c as a brown solid (86 mg; 33%). HPLC (UV), >99%; mp, 200 to 201°C. ^{1}H NMR (400 MHz, $CDCl_3$) δ 7.36 (d, J = 8.2, 4H, Ar*H*), 7.05 (d, J = 8.2, 4H, Ar*H*), 4.86 (s, 2H, O*CH*), 4.14 (m, 2H, OCH_2), 3.86 to 3.71 (m, 2H, NCH_2), 3.70 to 3.55 (m, 6H, NCH_2), 3.37 to 3.24 (m, 2H, OCH_2), 2.80 (s, 4H, PhCH_2), 1.98 to 1.73 (m, 4H, CH_2), 1.68 to 1.46 (m, 8H, CH_2). ^{13}C NMR (101 MHz, $CDCl_3$) δ 159.6 (2×C), 135.5 (2×C), 129.0 (2×C), 118.3 (2×C), 104.9 (2×C), 66.1 (2×C), 54.0 (2×C), 49.7 (2×C), 37.6 (2×C), 29.5 (2×C), 25.0 (2×C), 21.6 (2×C). LRMS (ESI^+) m/z = 549.56 (M + H).

(vi) N^2,N^6-bis(1-ethoxy-4,5-dihydro-1*H*-imidazol-2-yl)-9,10-dihydroanthracene-2,6-diamine (17b). The reaction was carried out by following the general procedure with 13b (615 mg; 0.64 mmol), thiophenol (0.39 ml; 3.85 mmol), and K_2CO_3 (1.06 g; 7.72 mmol) at room temperature for 7 days. Purification by silica chromatography as described above yielded 17b as a brown solid (30 mg; 11%). HPLC (UV), 92%; mp, 125 to 127°C. ^{1}H NMR (300 MHz, $CDCl_3$) δ 7.38 (s, 2H, Ar*H*), 7.13 (s, 4H, Ar*H*), 5.72 (m, 2H, *NH*), 3.96 (q, J = 7.0, 4H, OCH_2), 3.83 (s, 4H, CH_2), 3.57 (m, 4H, CH_2), 3.39 (m, 4H, CH_2), 1.27 (d, J = 7.0, 6H, CH_3). ^{13}C NMR (75 MHz, $CDCl_3$) δ 159.2 (2×C = N), 138.7 (2×Ar-*C*), 137.7 (2×Ar-*C*), 130.9 (2×Ar-*C*), 127.9 (2×Ar-*CH*) 118.5 (2×Ar-*CH*), 117.4 (2×Ar-*CH*), 70.8 (2×O-CH_2), 52.9 (2×CH_2), 47.0 (2×CH_2), 35.7 (2×CH_2), 14.3 (2×CH_3). LRMS (ESI^+) m/z = 435.32 (M + H).

(vii) N^2,N^6-bis(1-((tetrahydro-2*H*-pyran-2-yl)oxy)-4,5-dihydro-1*H*-imidazol-2-yl)-9,10-dihydroanthracene-2,6-diamine (17c). The reaction was carried out by following the general procedure with 13c (800 mg; 0.81 mmol), thiophenol (0.5 ml, 4.87 mmol), and K_2CO_3 (1.34 g; 9.74 mmol) at room temperature for 10 days. Purification by silica chromatography as described above yielded 17c as a brown solid (188 mg; 43%). HPLC (UV), 90%; mp, 130 to 132°C; ^{1}H NMR (400 MHz, $CDCl_3$) δ 7.7 (s, 2H), 7.34 (s, 4H, Ar*H*), 7.11 (s, 2H, Ar*H*), 5.1 (m, 2H, O*CH*), 4.0 (m, 2H, OCH_2), 3.70 (s, 4H, CH_2), 1.8 (m, 4H) 1.6 (m, 8H, CH_2). ^{13}C NMR (101 MHz, DMSO) δ 160.0 (2×C = N), 155.0 (2×C), 137.9 (Ar-*C*), 135.1 (Ar-*C*), 132.4 (2×Ar-*CH*), 128.8 (Ar-*C*), 128.4 (2×Ar-*CH*), 127.7 (Ar-*C*), 127.2 (Ar-*CH*), 124.0 (Ar-*CH*), 103.4 (2×*CH*), 62.2 (2×CH_2), 52.8 (2×CH_2), 41.1 (2×CH_2), 34.8 (2×CH_2), 27.3 (2×CH_2), 24.5 (2×CH_2), 18.5 (2×CH_2). LRMS (ESI^+) m/z = 547.41 (M + H).

General procedure for 2-tetrahydropyranyl (THP) group removal. A stirred solution of 14c to 17c in MeOH (1 ml) was treated with HCl gas (HCl_g)-saturated dioxane solution (3 ml). The reaction mixture was stirred at room temperature overnight, and the volatiles were evaporated under vacuum. Compounds 14d, 15d, and 17d were recrystallized from MeOH-acetone and rinsed with Et_2O. Compound 16d was recrystallized from isopropanol and rinsed with Et_2O.

(i) 4-((1-Hydroxy-4,5-dihydro-1*H*-imidazol-2-yl)amino)-*N*-(4-((1-hydroxy-4,5-dihydro-1*H*-imidazol-2-yl)amino)phenyl)benzamide (14d). Compound 14c (130 mg; 0.238 mmol) was treated as described above to yield 14d as a white solid (91.6 mg; 97%). HPLC (UV), >99%; mp, 164 to 165°C. Results for the dihydrochloride salt of 14d were the following: ^{1}H NMR (400 MHz, DMSO) δ 11.15 (s, 1H, *NH*), 11.09 (s, 1H, *OH*), 11.01 (s, 1H, *NH*), 10.77 (s, 1H, *NH*), 10.72 (s, 1H, *NH*), 9.36 (s, 1H,

OH), 9.02 (s, 1H, *NH*), 8.16 (d, $J = 8.7$, 2H, Ar*H*), 7.96 (d, $J = 8.9$, 2H, Ar*H*), 7.51 (d, $J = 8.7$, 2H, Ar*H*), 7.32 (d, $J = 8.9$, 2H, Ar*H*), 3.82 to 3.70 (m, 4H, NCH_2), 3.65 to 3.52 (m, 4H, NCH_2). ^{13}C NMR (101 MHz, DMSO) δ 164.6 (*C* = O), 160.1 (*C* = N), 159.5(*C* = N), 138.22 (Ar-*C*), 132.19 (Ar-*C*) 132.2 (Ar-*C*), 130.2 (Ar-*C*), 129.3 (2×Ar-*CH*), 124.8 (2×Ar-*CH*), 123.2 (2×Ar-*CH*), 121.3 (2×Ar-*CH*), 52.0 (NCH_2), 51.8 (NCH_2), 40.6 (NCH_2), 40.4 (NCH_2). LRMS (ESI$^+$) m/z = 396.33 (M + H). HRMS (ESI$^+$) $C_{19}H_{21}N_7O_3$ requires 395.1706 (found: 395.1720).

(ii) 1,3-Bis(4-((1-hydroxy-4,5-dihydro-1*H*-imidazol-2-yl)amino)phenyl)urea (15d). Compound 15c (10 mg; 0.017 mmol) was treated as described above to yield 15d as a brown solid (6 mg; 84%). HPLC (UV), 96%; mp, 170 to 175°C. Results for the dihydrochloride salt of 15d were the following: ^{1}H NMR (300 MHz, DMSO) δ 10.79 (s, 2H, *NH*), 10.64 (s, 2H, *NH*), 9.65 (s, 2H, *OH*), 8.89 (s, 2H, *NH*), 7.55 (d, $J = 8.6$, 4H, Ar*H*), 7.25 (d, $J = 8.6$, 4H, Ar*H*), 3.78 to 3.62 (m, 4H, NCH_2), 3.60 to 3.45 (m, 4H, NCH_2). ^{13}C NMR (101 MHz, DMSO) δ 160.3 (*C* = O), 152.7 (2×*C* = N), 139.0 (2×Ar-*C*), 128.2 (2×Ar-*C*), 125.5 (2×Ar-*CH*), 118.4 (2×Ar-*CH*), 52.1 (2×CH_2), 48.6 (2×CH_2). LRMS (ESI$^+$) m/z = 411.31 (M + H). HRMS (ESI$^+$) $C_{19}H_{22}N_8O_3$ requires 410.1815 (found: 410.1807).

(iii) 2,2′-((Ethane-1,2-diylbis(4,1-phenylene))bis(azanediyl)) bis(4,5-dihydro-1*H*-imidazol-1-ol) (16d). Compound 16c (50 mg; 0.091 mmol) was treated as described above to yield 16d as a brown solid (23.7 mg; 68%). HPLC (UV), 95%; mp, >224°C (decompose). Results for the dihydrochloride salt of 16d were the following: ^{1}H NMR (400 MHz, DMSO) δ 11.04 (s, 2H, *OH*), 10.77 (s, 2H, N*H*), 9.00 (s, 2H, N*H*), 7.35 (d, $J = 7.8$, 4H, Ar*H*), 7.26 (d, $J = 7.8$, 4H, Ar*H*), 3.73 (t, $J = 7.7$, 4H, NCH_2), 3.54 (t, $J = 7.7$, 4H, NCH_2), 2.91 (s, 4H, CH_2). ^{13}C NMR (101 MHz, DMSO) δ 159.9 (2×*C* = N), 140.3 (2×Ar-*C*), 132.9 (2×Ar-*C*), 129.5 (4×Ar-*CH*), 124.1 (4×Ar-*CH*), 51.9 (2×NCH_2), 40.5 (2×NCH_2), 36.2 (2×CH_2). LRMS (ESI$^+$) m/z = 381.43 (M + H). HRMS (ESI$^+$) $C_{20}H_{24}N_6O_2$ requires 381.1961 (found: 381.1585).

(iv) 2,2′-((9,10-Dihydroanthracene-2,6-diyl)bis(azanediyl))bis(4,5-dihydro-1*H*-imidazol-1-ol) (17d). Compound 17c (96 mg; 0.18 mmol) was treated as described above to yield 17d as a light brown solid (45.9 mg; 69%). HPLC (UV), 97%; mp, >130°C (decompose). Results for the dihydrochloride salt of 17d were the following: ^{1}H NMR (300 MHz, DMSO) δ 10.80 (br s, 2H, N*H*), 10.77 (s, 2H, N*H*), 8.92 (br s, 2H, O*H*), 7.43 (d, $J = 8.0$, 2H, Ar*H*), 7.33 (d, $J = 2.0$, 2H, Ar*H*), 7.17 (dd, $J = 8.0, 2.0$, 2H, Ar*H*), 3.96 (s, 4H, CH_2), 3.77 to 3.67 (m, 4H, NCH_2), 3.60 to 3.51 (m, 4H, NCH_2). ^{13}C NMR (101 MHz, DMSO) δ 159.6 (2×*C* = N), 148.7 (2×Ar-*C*), 138.6 (Ar-*C*), 136.1 (Ar-*C*), 132.7 (2×Ar-*CH*), 129.2 (Ar-*C*), 128.1 (2×Ar-*CH*), 125.4 (Ar-*C*), 123.5 (Ar-*CH*), 122.7 (Ar-*CH*), 50.3 (2×NCH_2), 44.0 (2×NCH_2), 36.2 (2×CH_2). LRMS (ESI$^+$) m/z = 379.33 (M + H). HRMS (ESI$^+$) $C_{20}H_{22}N_6O_2$ requires 378.1804 (found: 378.1792).

Biology. (i) Cultivation of parasites, *in vitro* activity, and cytotoxicity. For all of the susceptibility assays with parasites and L6 cells, each compound was tested in duplicate and each assay was repeated at least once.

***(a)* Activity against *T. brucei*.** The *in vitro* trypanocidal and cytotoxic activities were determined using an alamarBlue-based assay (11, 12). Detailed experimental protocols for these assays with *T. b. rhodesiense* STIB900 and rat skeletal myoblast L6 cells (ATCC CRL-1458) have been reported before (13). A slight modification of this protocol (i.e., 5-fold higher parasite load and longer [24-h] incubation time with alamarBlue before reading) was used for the assays with wild-type (WT) and resistant *T. b. brucei* strains, as described previously (14). The TbAT1-KO strain is derived from the wild-type strain *T. b. brucei* Lister 427 (s427) by deletion of the *T. brucei AT1* (*TbAT1*) gene (15). The B48 strain is a mutant derived from TbAT1-KO by *in vitro* selection to high levels of pentamidine and does not express a functional high-affinity pentamidine transporter (HAPT1) (16). The STIB900 strain was isolated in 1982 from a human patient in Tanzania and, after several mouse passages, was cloned and adapted to axenic culture conditions (17, 18).

***(b)* Activity against *T. cruzi*, *Leishmania donovani*, and *Plasmodium falciparum*.** Fifty percent inhibitory concentrations (IC_{50}s) against amastigotes of *L. donovani* strain MHOM/ET/67/L82 were determined using an alamarBlue-based assay (11, 12). IC_{50}s against erythrocytic stages of *P. falciparum* was determined by a [^{3}H]hypoxanthine incorporation assay (19) using the chloroquine- and pyrimethamine-resistant strain K1, which originated from Thailand (20). IC_{50}s against amastigote forms of *T. cruzi* Tulahuen strain C2C4, containing the β-D-galactosidase (LacZ) gene, were determined using a colorimetric assay with the substrate chlorophenyl red β-D-galactopyranoside (CPRG)-Nonidet (21). Detailed experimental protocols for all of these assays have been reported before (13).

(ii) *In vivo* antitrypanosomal activity. *(a) T. b. rhodesiense* (STIB900) acute mouse model. The acute mouse model mimics the first stage of the disease. Four female NMRI mice were used per experimental group. Each mouse was inoculated i.p. with 10^4 bloodstream forms of STIB900, respectively. Heparinized blood from a donor mouse with parasitemia of approximately 5×10^6/ml was suspended in phosphate-buffered saline with glucose (PSG) to obtain a trypanosome suspension of 1×10^5/ml. Each mouse was injected with 0.25 ml. Compounds were formulated in 100% DMSO and diluted 10-fold in distilled water. Compound treatment was initiated 3 days postinfection on four consecutive days for both administration routes (i.p. and p.o.) in a volume of 0.1 ml/10 g. Four mice served as infected-untreated controls. They were not injected with the vehicle alone, since we have established in our laboratory, over many years, that these vehicles do not affect parasitemia or the mice (results not shown). Parasitemia was monitored using smears of tail-snip blood twice a week after treatment for 2 weeks, followed by once a week until 60 days postinfection. Mice were considered cured when there was no parasitemia relapse detected in the tail blood over the 60-day observation period. Mean relapse days (MRD) were determined as day of relapse postinfection of mice.

***(b) T. b. brucei* (GVR35) mouse CNS model.** The GVR35 strain was isolated from a wildebeest in the Serengeti in 1966 (primary isolate S10) (22). The GVR35 mouse CNS model mimics the second stage of the disease. Five female NMRI mice per experimental group were used. Each mouse was inoculated i.p. with 2×10^4 bloodstream forms. The treatment was i.p. in a volume of 10 ml kg^{-1} on five consecutive days from day 17 to 21 postinfection. A control group was treated on day 17 with a single dose of diminazene aceturate at 40 mg/kg i.p., which is subcurative, since it clears the trypanosomes only in the hemolymphatic system and not in the CNS, leading to the subsequent reappearance of trypanosomes in the blood (22). Parasitemia was monitored twice in the first week after treatment, followed by once a week until 180 days postinfection. Mice were considered cured when there was no parasitemia relapse detected in the tail blood over the 180-day observation period. Surviving mice were euthanized on day 180, and the day of death of the animals was recorded (including the cured mice, which were recorded as >180) to calculate the MRD.

All of the *in vivo* efficacy studies in mice (STIB900 and GVR35 models) were conducted at the Swiss Tropical and Public Health Institute (Basel) according to the rules and regulations for the protection of animal rights (Tierschutzverordnung) of the Swiss Bundesamt für Veterinärwesen. They were approved by the veterinary office of Canton Basel-Stadt, Switzerland.

(iii) *In vitro* BBB permeability studies. *(a)* Cell line culture. The hCMEC/D3 human cerebral endothelial monolayers were grown in EBM-2 medium (Lonza, Basel, Switzerland) supplemented with 5% fetal bovine serum Gold, 10 mM *N*-2-hydroxyethylpiperazine-*N*′-2-ethanesulfonic acid (HEPES; PAA Laboratories GmbH, Pasching, Austria), 1% penicillin-streptomycin, 1% chemically defined lipid concentrate (Invitrogen Ltd., Paisley, United Kingdom), 1.4 mM hydrocortisone, 5 mg/ml ascorbic acid, and 1 ng/ml basic fibroblast growth factor (bFGF) (Sigma-Aldrich, St. Louis, MO, USA). Cells were seeded at a density of 50,000 cells/cm^2 in Transwell culture inserts (0.4-mm pore size; Corning, Lowell, MA, USA) precoated with rat type I collagen (R&D Systems, Minneapolis,

MN, USA) and grown for 6 days at 37°C in a humidified incubator in 5% CO_2. The medium was changed 3 days after seeding.

***(b)* Permeability assays.** The compounds were dissolved in distilled water (10 mM stock solution), and the permeability assays were performed with the hCMEC/D3 human brain endothelial monolayer as described earlier (8). Prior to compound permeability studies, the working concentration of the compounds (i.e., concentration that does not disturb the cellular complex between endothelial cells) was determined using the fluorescent dye Lucifer yellow (LY; Sigma, St. Louis, MO, USA) as a marker of tight junction integrity. The working concentrations used were 100 μM for pentamidine, I, 14d, and III and 50 μM for V. Briefly, the experiments were run as follows. After 6 days of culture, coated culture inserts with and without endothelial cells were transferred to 6-well plates containing 2.6 ml of transport buffer (Hanks buffered saline solution with $CaCl_2$ and $MgCl_2$, 10 mM HEPES, 1 mM sodium pyruvate [Invitrogen Ltd., Paisley, United Kingdom], and, when required, 0.1% bovine serum albumin [BSA]) in the abluminal chamber. At time zero, transport buffer, containing tested compound with or without LY (50 μM dissolved in cell culture-tested water), was placed in each luminal chamber. Transport incubations occurred at 37°C, 95% humidity, and 5% CO_2. At different times (10, 25, and 45 min), each culture insert (with and without cells) was transferred to a new lower compartment containing fresh transport buffer. The amount of each compound in the lower compartments at different time points, in the upper one at the end of the experiment, and in the working solution was quantified either by fluorimetry (for LY) or by HPLC-MS (for compounds I, 14d, III, V, and pentamidine). Endothelial permeability was calculated from the clearance rate and the surface area, as previously described (8, 23, 24). Data represent means from three independent culture inserts per condition.

To temporarily destroy tight junctions between cerebral endothelial cells, a hyperosmotic solution of D-mannitol (1.4 M in EBM-2) was applied to cells 30 min prior to permeability studies.

***(c)* HPLC analysis of the results.** One-ml samples for each time point were taken directly from the basal compartment and transferred to 1.5-ml Waters HPLC vials that were stored in the freezer. The samples were defrosted and stored at 4°C the day before the HPLC analysis. The samples were shaken with an orbital shaker for 40 min, and the analytical HPLC was run with a Waters Sunfire C_{18}, 3.5-μm (4.6- by 50-mm) column on a Waters 2690 separation module with a Waters 996 photodiode array detector. The following HPLC conditions were used: column temperature, 30°C; flow rate, 1 ml/min; volume of injection, 10 μl. The solvent mixture was H_2O (+0.05% CF_3CO_2H):CH_3CN (+0.05% CF_3CO_2H), with the following proportions: pentamidine (isocratic, 20:80; gradient time, 10 min), I (isocratic, 10:90; gradient time, 5 min), 14d (isocratic, 7:93; gradient time, 5 min), III (isocratic, 15:85; gradient time, 5 min), and V (isocratic, 10:20; gradient time, 5 min). The analytical wavelength was 262 nm (pentamidine), 275 nm (compounds I and 14d), 234 nm (compound III), and 280 nm (compound V). Each sample was injected 3 times, and the mean value of the compound UV peak area was used to determine the concentration of the sample according to the calibration curves. Calibration curves were obtained for each compound using 6 different concentrations obtained by serial double dilution in the assay buffer starting from 150 μM for pentamidine, I, III, and V or 120 μM for 14d. Each concentration was tested in triplicate, and the mean value of the compound UV peak area versus concentration was plotted. The equation for the calibration curve was obtained by linear regression analysis using the Microsoft Excel program.

Physicochemical studies. (i) pK_a determination by UV-visible spectrophotometry. Ionization constants were measured by UV spectrophotometry using 96-well microtiter plates as described elsewhere (25). The method consists of the simultaneous determination of the compound's UV spectrum as a function of pH. The compounds in stock solution in DMSO are dissolved in different aqueous buffer solutions directly in the microtiter plate (the maximum amount of DMSO in the final solution is 2%, vol/vol). Further treatment of the data generates the pK_a values in a medium-throughput manner. All of the pK_a values were measured at 30°C, at a concentration of 0.2 mM, and at constant ionic strength ($I = 0.1$ M).

(ii) SPR biosensor measurements of HSA binding. Surface plasmon resonance (SPR) experiments were performed at 25°C with a Biacore X-100 apparatus (GE Healthcare, Biacore AB, Uppsala, Sweden).

***(a)* Immobilization of HSA.** Essentially fatty acid- and globulin-free HSA (Sigma-Aldrich) was used without further purification. A stock solution was prepared in phosphate-buffered saline (PBS; pH 7.4) and stored at −20°C. Immediately prior to use, this solution was diluted to a concentration of 100 μg/ml in 10 mM sodium acetate, pH 5.0. HSA was immobilized on CM5 sensor chips (Biacore) by the use of amine-coupling chemistry. The surface was blocked by a 7-min injection with 1 M ethanolamine, pH 8.0. The immobilization level ranged between 8,000 and 9,000 response units (RU).

***(b)* Ranking experiments.** Control drugs (warfarin, phenytoin, prednisone, and sulfanilamide) and compounds I, 14a, 14d, 15e, 16b, 16d, IV, and V were prepared as 10 mM stock solutions in 100% DMSO. The stock solutions were diluted in PBS containing DMSO to reach a final concentration of 40 μM in PBS containing 3% DMSO. Binding studies were performed at a flow rate of 90 μl/min with 40-s association and 60-s dissociation times. Regeneration was not required between injection cycles. To clean the flow system, an extra wash with 50% DMSO was performed between each injection. Binding responses were corrected for solvent (DMSO bulk differences) by using the software available on the Biacore X-100 instrument. Several measurements of warfarin binding to HSA were carried out over the course of the experiment as a means of the control of the HSA binding efficiency throughout the assay. The dose-response curves were obtained by plotting the RU/Da × 100 against the drug concentrations. At a working concentration (40 μM), all of the compounds gave measurable responses. Positive controls were used, ranking from warfarin to prednisone, and the graph of HSA binding levels could be divided into regions of low, intermediate, and high binding responses (see Fig. 3). Sulfanilamide was a negative control, as it hardly binds to HSA.

RESULTS

Chemistry. The lead compounds I to V (Fig. 1) were synthesized as previously reported (9, 26). Their spectroscopic and analytical data were in agreement with the reported ones. The *N*-alkoxy derivatives 14 to 17e were synthesized in 3 steps from the corresponding diamines 1 to 4 by following a protocol developed previously in our laboratory (Fig. 2) (8, 27). Diamines 1 to 4 were converted to the isothiocyanates 5 to 8 in high yield using thiophosgene in H_2O-Et_2O. The addition of 2 equivalents of the *N*-(2-aminoethyl)-*N*-alkoxy-2-nitrobenzenesulfonamide reagent 9 (27) to 5 to 8 gave the thioureas 10 to 13. Some of these intermediate thioureas were isolated by crystallization or silica chromatography (compounds 10c, 11a, 11c, 12b and c, and 13b and c), whereas the others (10a and b, 11b, 11d, 12a, and 13a) were detected by HPLC-MS in the reaction, and the crude product was used as such in the next steps. Nosyl group removal and intramolecular cyclization to generate the imidazoline target compounds 14a to 17e were performed either with a one-pot procedure (compounds 14a and b, 15b, 15d, 16a, and 17a) or in two steps (compounds 14c, 15a, 15c, 16b, 16c, and 17c) with the isolation of the intermediate thiourea (see below). Compound 17a was contaminated with approximately 20% of anthracene 18a, which probably results from the competitive oxidation of the intermediates (13a and/or 17a) during the deprotection-cyclization steps in the presence of sulfur reagent (28). Since we were not able to separate both compounds, 17a was assayed as a mixture. The *N*-hydroxy deriv-

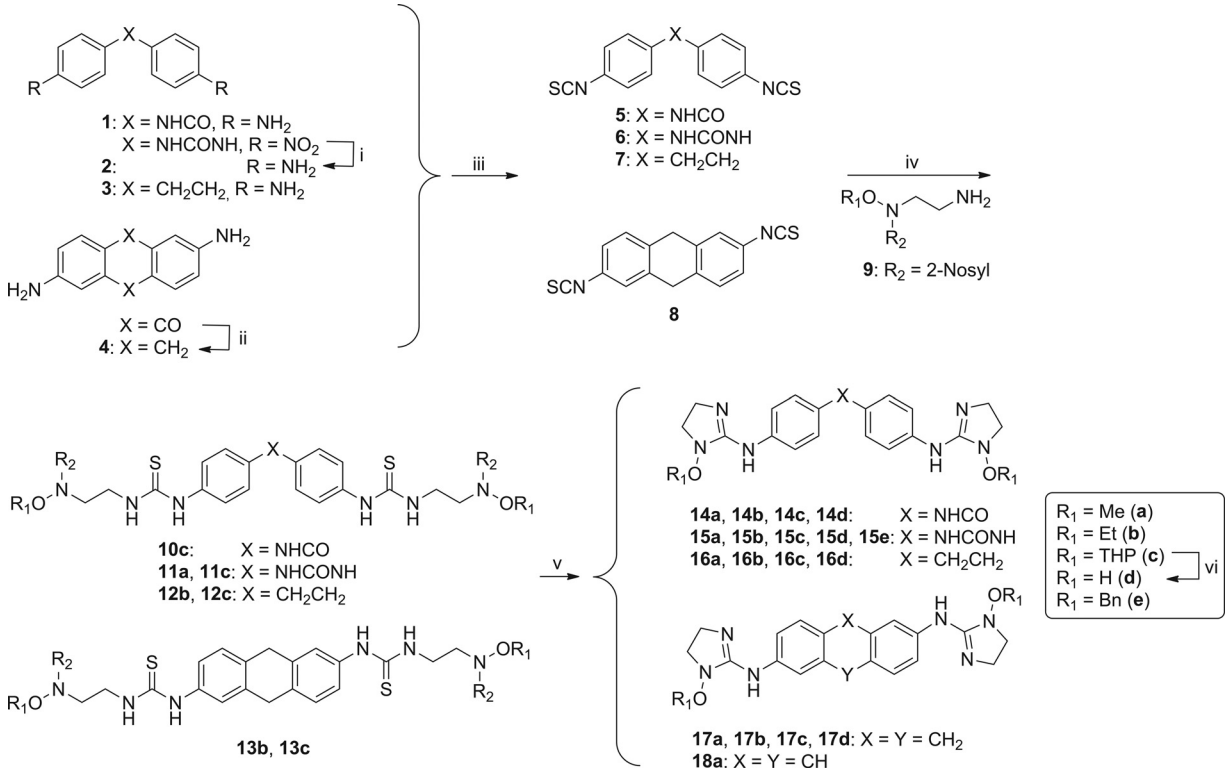

FIG 2 Synthesis of 1-alkoxy-2-arylaminoimidazolines. Reagents and conditions include the following: (i) H_2, 5% Pd-C, MeOH, room temperature; (ii) activated Zn, NH_3, sealed tube, 100°C; (iii) thiophosgene, H_2O-ether, room temperature; (iv) 9 (2 equiv), DMF, room temperature; (v) Step 1: PhSH (6 equiv), K_2CO_3 (12 equiv), DMF, room temperature; step 2: 50°C; (vi) HCl_g/dioxane, MeOH, room temperature.

atives 14d to 17d were obtained smoothly as hydrochloride salts by acidic hydrolysis of the THP-protected precursors 14c to 17c.

***In vitro* antiprotozoal activity.** The *N*-alkoxy and *N*-hydroxy derivatives 14 to 17e were assayed *in vitro* against *T. brucei rhodesiense* using an alamarBlue-based assay (11). Their cytotoxicity against mammalian cells (i.e., rat L6 cells) also was evaluated. In addition, the compounds were screened against other related parasites (*T. cruzi*, *L. donovani*, and *P. falciparum*). The new compounds showed little activity against *T. cruzi* or *L. donovani* amastigotes and moderate activities (IC_{50}s in the range of 0.6 to 6.3 μM) against the chloroquine/pyrimethamine-resistant strain of *P. falciparum*. These values represent a >30-fold loss of activity against *P. falciparum* compared to that of the lead compounds I to V (Table 1). In contrast, eight compounds (14d, 15d, 15e, 16a to 16d, and 17c) showed low-micromolar IC_{50}s (≤10 μM) against *T. brucei* trypomastigotes, four compounds (14a to 14c and 15c) had IC_{50}s in the range of 10 to 20 μM, and two compounds (15a and 15b) displayed poor activity (>20 μM) (Table 1). These values represent a 20- to 160-fold loss of activity against *T. b. rhodesiense* versus the lead compounds I to V. Some general trends were observed regarding the *in vitro* anti-*T. brucei* activity of the *N*-OR derivatives. The influence of the *N*-substituent in order of decreasing activity was OBn > OH > OTHP > OEt > OMe. Importantly, compounds with OH substituents were less cytotoxic than the rest of the molecules, including the parent lead compounds, and showed the best selectivity indices among the new compounds. In contrast, the *N*-OTHP analogues (14c to 17c) were the most cytotoxic from each series. The *N*-hydroxy derivative 14d displayed the best *in vitro* efficacy against *T. brucei*, with a submicromolar IC_{50} (0.89 μM) and excellent selectivity (SI of >240) for the parasite.

***In vitro* activity against drug-resistant *T. brucei* strains.** Cross-resistance with existing trypanocidal drugs, such as pentamidine and melarsoprol, is a drawback that is commonly observed with diamidine-like compounds. Diamidines are substrates of the *Tb*AT1/P2 aminopurine transporter (29) and of the high- and low-affinity pentamidine transporters (HAPT and LAPT, respectively) (30). The loss of one or more of these transporters has been linked to cross-resistance between arsenicals and diamidine drugs (31). Since our compounds are diamidine-like and hold the P2 transporter recognition motif (32), we tested their activity against two different drug-resistant strains of trypanosomes (i.e., TbAT1-KO and B48). Hence, the most active analogue, 14d, and its parent compound, I, were tested against WT and drug-resistant strains of *T. brucei* to establish their resistance profile. Parent compound I was approximately 5-fold more active against the wild type than against either of the drug-resistant *T. b. brucei* strains (Table 2), indicating that the cellular uptake of this compound is partly dependent on the *Tb*AT1 transporter (compare the WT to the TbAT1-KO strain), whereas the expression of HAPT1 did not appear to influence sensitivity to these compounds (compare TbAT1-KO to B48). In contrast, 14d showed similar activity against the three *T. brucei* strains, indicating that these transporters are not essential for the uptake of this compound *in vitro*. We conclude that I is dependent on the presence of transporters for uptake across biological membranes, as the absence of *Tb*AT1 in trypanosomes reduces its activity. In contrast,

TABLE 1 *In vitro* antiprotozoal activity of *N*-alkoxy and *N*-hydroxy analogues of the lead compounds I to V

Compound	IC_{50} (μM) for[a]: *T. b. rhodesiense*	*T. cruzi*	*L. donovani*	*P. falciparum*	Cytotoxicity [CC_{50} (μM)] for L6 cells[b]	SI[c]
I[d]	0.025 ± 0.002	ND[e]	ND	0.028 ± 0.005	193 ± 23	7720
14a	18.4 ± 4.3	152 ± 9	41.6 ± 1.4	1.04 ± 0.03	75.8 ± 0.1	4
14b	11.6 ± 1	130 ± 8	15.9 ± 2.7	1.34 ± 0.05	102 ± 6	8.8
14c	16.7 ± 7.6	37.7 ± 3.3	92 ± 2.3	2.2 ± 0.9	26.1 ± 1.3	1.5
14d	0.89 ± 0.07	161 ± 29	>213	1.7 ± 0.4	>213	>240
II[d]	0.122 ± 0.004	ND	ND	0.028 ± 0.009	104 ± 9	852
15a	150 ± 2	>228	171 ± 81	5.1 ± 0.5	113 ± 57	0.7
15b	45.9 ± 0.9	>192	96 ± 10	6.3 ± 1.2	>192	>4
15c	19.5 ± 12.8	131 ± 41	88.3 ± 7.4	1.9 ± 0.6	23.2 ± 10.4	1.2
15d	7.9 ± 3.8	108 ± 3	>206	2.8 ± 0.7	>206	>26
15e	2.4 ± 0.3	13.7 ± 7.3	1.0 ± 0.2	4.6 ± 0.6	30.9 ± 0.3	12.8
III[d]	0.054 ± 0.004	ND	ND	0.016 ± 0.003	34.9 ± 13.1	646
16a	10.9 ± 2.5	32 ± 7	138 ± 57	1.05 ± 0.2	77.7 ± 0.8	7
16b	4.4 ± 0.1	41.5 ± 2.5	123 ± 60	0.826 ± 0.002	49.7 ± 3.2	11
16c	3.2 ± 0.6	7.8 ± 3.0	98 ± 41	0.56 ± 0.08	11.1 ± 9.6	2.8
16d	5.4 ± 0.4	111 ± 14	179 ± 59	0.64 ± 0.23	88.3 ± 14.6	16.5
IV[d]	0.060 ± 0.025	ND	ND	0.019 ± 0.001	37.3 ± 5.2	620
17c[f]	3.5 ± 1	26 ± 0.3	45.6 ± 12.1	0.60 ± 0.02	19.1 ± 0.2	5.4
V[d]	0.005 ± 0.001	ND	ND	0.011 ± 0.001	83.4 ± 20.6	17020
Melarsoprol	0.005 ± 0.003					
Benznidazole		1.35 ± 0.28				
Miltefosine			0.53 ± 0.17			
Chloroquine				0.13 ± 0.04		
Podophyllotoxin					0.012 ± 0.005	

[a] IC_{50} ± standard deviations (SD) are given (averages from two independent assays). *T. brucei rhodesiense* STIB900 trypomastigotes, *T. cruzi* Tulahuen strain C2C4 intracellular amastigotes, axenically grown *L. donovani* strain MHOM/ET/67/L82 amastigotes, and *P. falciparum* K1 strain erythrocytic stages were used.
[b] Rat skeletal myoblast L6 cells.
[c] The selectivity index was calculated as (CC_{50} for L6 cells)/(IC_{50} for *T. b. rhodesiense*).
[d] Data were reported previously in reference 9 and are included here for comparative purposes.
[e] ND, not determined.
[f] Compounds 17a, 17b, and 17d were not tested *in vitro*.

14d diffuses in a transporter-independent fashion across the same membranes.

***In vivo* antitrypanosomal activity. (i) Mouse model of acute HAT.** The *in vivo* efficacy of the new derivatives displaying the best *in vitro* activities and selectivity (i.e., IC_{50} of <15 μM and SI of >5) was checked in the STIB900 murine model of sleeping sickness (Table 3). In this stringent stage 1 model, mice infected with *T. b. rhodesiense* parasites develop an acute hemolymphatic infection that is difficult to cure. Each compound was administered to groups of 4 mice in a 4-day schedule by either the oral (p.o.) or intraperitoneal (i.p.) route. The mean day of relapse of parasitemia and the number of animals cured (i.e., animals that survived and were parasite free for 60 days) was calculated for each group (Table 3). The lead compounds were very effective in this model, as they were curative with i.p. dosages as low as 5 mg/kg (I, II, and V) and 10 mg/kg (III and IV). Moreover, compounds I and V also were curative by the oral route at 50 mg/kg/day p.o. Among the new compounds, the methoxy (16a and 17a), ethoxy (14b and 16b), and benzyloxy (15e) derivatives were inactive both by intraperitoneal and oral routes. In this series, the most active molecules were the hydroxy derivatives (14d, 17d, 15d, and 16d), which were able to increase moderately the mean day of relapse of parasitemia

TABLE 2 *In vitro* activity against WT and drug-resistant *T. brucei* strains

Compound	Findings for: WT[a] IC_{50} (μM)	*n*	TbAT1-KO[b] IC_{50} (μM)	*n*	RF[c]	B48[d] IC_{50} (μM)	*n*	RF
I	5.70 ± 0.96	3	25.5 ± 3.5	3	4.5	29.6 ± 3.6	3	5.2
14d	15.5 ± 2.0	3	17.1 ± 1.9	3	1.1	18.6 ± 2.1	3	1.2
Pentamidine	0.006 ± 0.002	3	0.011 ± 0.002	3	1.8	0.543 ± 0.014	3	90.5
Diminazene	0.148 ± 0.011	3	0.738 ± 0.066	3	5.0	0.736 ± 0.209	3	5.0

[a] *T. b. brucei* 427 trypomastigotes. Values represent IC_{50} ± standard errors of the means (SEM) ($n \geq 3$).
[b] *T. b. brucei* knockout strain lacking a functional P2 transporter and resistant to diminazene aceturate (15).
[c] Resistance factor compared to the WT.
[d] The B48 strain is a mutant derived from the TbAT1-KO strain with a nonfunctional high-affinity pentamidine transporter (HAPT). This strain is resistant to diminazene, pentamidine, and melaminophenyl arsenicals (16).

TABLE 3 *In vivo* antitrypanosomal activity of lead compounds and *N*-substituted analogues in the *T. b. rhodesiense* (STIB900) mouse model[a]

Compound	R	Dosing route[b]	Dosage (mg/kg)	No. cured[c]/ no. infected	Mean day (±SD) of relapse[d]
Control				0/4	7[e]
I	H	i.p.	4 × 20[f]	**4/4**	**>60**
		i.p.	4 ×10	**4/4**	**>60**
		i.p.	4 × 5	**4/4**	**>60**
		p.o.	4 × 50	**4/4**	**>60**
14d	OH	i.p.	4 × 50	**4/4**	**>60**
		i.p.	4 × 20	**4/4**	**>60**
		i.p.	4 × 10	**1/4**	**>31**
		i.p.	4 × 5	0/4	20.5 ± 4.7
		p.o.	4 × 50	0/4	10.5 ± 4.0
II	H	i.p.	4 × 20[f]	**4/4**	**>60**
		i.p.	4 ×10	**2/4**	**60**
		i.p.	4 × 5	**3/4**	**60**
		p.o.	4 × 50	0/4	9.5 ± 5.0
15d	OH	i.p.	4 × 40	0/4	12.7 ± 5.6
15e	OBn	i.p.	4 × 50	0/4	7
		p.o.	4 ×100	0/4	7
III	H	i.p.	4 × 20[f]	**4/4**	**>60**
		i.p.	4 ×10	**1/4**	46.7 ± 24.8
		i.p.	4 × 5	0/4	15.7 ± 3.5
		p.o.	4 × 50	0/4	7
16b	OEt	i.p.	4 × 30	0/4	7
		p.o.	4 ×50	0/4	7.7 ± 1.5
16d	OH	i.p.	4 × 50	0/4	14 ± 0
IV	H	i.p.	4 × 20[f]	**4/4**	**>60**
		i.p.	4 ×10	**3/4**	**>60**
		i.p.	4 × 5	0/4	25.5 ± 23
		p.o.	4 × 50	0/4	13.0 ± 2.0
		p.o.	4 × 20	0/4	7.7 ± 1.5
		p.o.	4 × 10	0/4	9.2 ± 1.5
17d	OH	i.p.	4 × 20	0/4	18.3 ± 5.1
		p.o.	4 × 50	0/4	7
V	H	i.p.	4 × 20	**4/4**	**>60**
		i.p.	4 × 10	**3/3**[g]	**>60**
		i.p.	4 × 5	**4/4**	**>60**
		p.o.	4 × 50	**3/4**	**>50**
Melarsorpol[h]		i.p.	4 × 2	4/4	>60
Pentamidine[h]		i.p.	4 × 5	1/4	>38

[a] See Materials and Methods for details of the STIB900 (*T. b. rhodesiense*) model. Boldface values are for compounds that were able to cure one or more mice.
[b] i.p., intraperitoneal; p.o., per os.
[c] Number of mice that survived and were parasite free for 60 days.
[d] Average day of relapse of parasitemia.
[e] Control mice were always positive and were euthanized on day 7.
[f] The *in vivo* activity at 20 mg/kg i.p. was reported previously in reference 9; the dose-response experiments at lower dosages (i.p. and p.o.) are reported here for the first time.
[g] One mouse died during treatment (day 4).
[h] Data reported in reference 61.

at 5, 20, 40, and 50 mg/kg/day i.p., respectively. The *N*-hydroxy analogue 14d was 100% curative in this model, with a dosage as low as 20 mg/kg i.p. Oral administration was only weakly effective at the dose tested (50 mg/kg).

(ii) Mouse model of chronic (CNS-stage) HAT. The capacity of the lead compounds I to V and the most active derivative, 14d, to cure the CNS stage of the disease was investigated using the GVR35 mouse model. In this model of chronic infection, trypanosomes have invaded the brains of the animals and are present in the cerebrospinal fluid (22). To cure this stage of trypanosomiasis, the drugs must be able to cross the BBB. In these experiments, diminazene aceturate, a very efficient trypanocidal drug for stage 1 animal trypanosomiasis, was used as a negative control, as it is unable to penetrate into the brain. In contrast, melarsoprol cures this mouse model at a dose of 15 mg/kg given by the intraperitoneal route on 5 consecutive days (33). As shown in Table 4, the lead compounds I to IV were inactive in this model, as a dosage of 50 mg/kg i.p. for 5 days gave no better protection than diminazene aceturate. In contrast, the lead compound V increased by 131% the mean parasite-free survival time, T_S, compared to that of control animals treated with diminazene aceturate ($P < 0.01$), indicating modest brain permeation.

The hydroxy derivative 14d was inactive in this model of CNS infection when administered at a dose of 5 × 40 mg/kg/day i.p. However, in another experiment, using a higher dose and different treatment regimen (100 mg/kg/day i.p. given as a twice-daily dose of 50 mg/kg), 14d increased its T_S to 143% of that of the control ($P < 0.01$), although no cures were obtained (Table 4). Altogether, the *in vivo* results indicate that the *N*-hydroxy derivative 14d is safer than I (i.e., a higher dosage is tolerated) and exhibits improved activity against brain infection with trypanosomes.

Physicochemical properties: pK_a determination. The pK_a of a drug is an essential physicochemical parameter that gives information on the ionization state of the molecule at physiological pH. Knowledge of this parameter is important, because the bis-2-aminoimidazoline lead compounds I to V are dibasic molecules (pK_a in the range of 9.29 to 10.71) that will be dications at pH 7.4. This may result in poor diffusion across the BBB, which may explain in part their poor efficacy in the CNS stage of the disease compared to the early-stage model. Our intention when synthesizing *N*-alkoxy and *N*-hydroxy derivatives was to reduce the pK_a of these leads to decrease the proportion of the ionized form of the compounds in biological fluids.

The pK_a values of these dibasic compounds were measured by UV spectrophotometry in a medium-throughput manner using a 96-well microtiter plate-based protocol recently developed by our group (25). The results of experimental pK_a as well as other calculated physicochemical properties are shown in Table 5. The introduction of O-alkoxy substituents on the imidazoline nitrogen reduced the basicity of the lead compounds by approximately 2 pK_a units, as expected. However, the nature of the O-alkyl substituent did not alter the pK_a within the homologous series (e.g., compare 14a to 14d). The pK_a of *N*-OR-substituted *N*-phenylbenzamide derivatives (14a to d) is in the range of 7.2 to 7.4. Hence, these compounds will be approximately 50% ionized at physiological pH (Table 5), whereas the pK_a of the urea and ethylene derivatives (15a to b and 16a to d, respectively) is about 0.5 pK_a units higher, which means approximately 80% ionization under physiological conditions.

SPR-biosensor analysis of serum protein binding. HSA is one

TABLE 4 *In vivo* antitrypanosomal activity in the chronic (CNS-stage) phase of infection[a]

Compound	Dosage (mg/kg)	No. cured/no. infected	Mean day of relapse (control group)	T_S (% of control)	*P* value[h]
Diminazene aceturate	1 × 40	0/5	46.6 ± 5.1 (1) 36.8 ± 3.2 (2) 37.5 ± 6.1 (3)	100	
I	5 × 50	T[b]	T[b] (1)	108	NA
	5 × 20	0/5	51.2 ± 6.7 (1)		0.26
14d	5 × 40	1/4[c]	45.0 ± 5.6[c] (1)	98	0.69
	5 × 100[d]	0/4[e]	52.2 ± 9.5[f] (2)	143	0.0052
II	5 × 50	T[b]	T[b] (1)	91	NA
	5 × 20	0/5	42.8 ± 7.9 (1)		0.39
III	5 × 50	0/5[g]	40 ± 1.7 (1)	85	0.081
IV	5 × 50	0/5[g]	43 ± 5.3 (1)	91	0.38
V	5 × 50	0/4[e]	49 ± 0 (3)	131	0.0035

[a] Summary of three experiments using the GVR35 mouse model of late-stage trypanosomiasis. All administrations were by the intraperitoneal route; diminazene treatment was used as a control, and the controls for the three experiments are given separately, representing average days of relapse of parasitemia ± SD for 5 (control 1) or 6 (controls 2 and 3) mice. All treatments were initiated on day 17 postinfection (p.i.). Mice that survived and remained parasite free after treatment up to 180 days p.i. were considered cured.
[b] All mice died after the 4th treatment (T, terminated), assumed to be due to the toxicity of the compound.
[c] In this experiment, 3 mice relapsed, on days 39, 46, and 50 (not statistically different from control 1), and one mouse survived as infection negative for 180 days but was discarded from the calculation of the MDR as a probable outlier.
[d] Compound given as a twice-daily dose of 50 mg/kg.
[e] One mouse died during treatment and was excluded from the experiment.
[f] In this experiment, 4 mice relapsed on days 51, 51, 42, and 65.
[g] Two mice died during treatment, assumed to be due to the toxicity of the compound.
[h] Statistical significance was assessed for each group against their control group using an unpaired Student *t* test. NA, not applicable.

of the most relevant plasma proteins affecting drug distribution in the body (34). HSA plays a critical role in transporting drugs, metabolites, and endogenous ligands (35). Since high binding to plasma protein reduces the free drug concentration, decreased antiparasitic activity is expected for high-level HSA binders. Some classes of antibiotics, for instance, provide well-documented examples of this relationship between antimicrobial activity and the unbound concentration at the site of infection (36). Hence, knowing the binding levels of our compounds to HSA should provide essential information to anticipate their pharmacokinetic behavior in humans. In the present study, the amount of compound binding to HSA at a single concentration (40 μM) was determined by SPR-biosensor binding experiments using previously reported protocols (37, 38). Four drugs with different levels of binding to

TABLE 5 Calculated physicochemical parameters and experimental ionization constants

Compound	Molecular wt[a]	HBD	clog*P*[a]	log$D_{7.4}$[a,b]	PSA[a] (Å^2)	Exptl pK_a[c]	% ionization at pH 7.4
I	363	6	1.67	−1.2	101.94	9.29 ± 0.07[d]	98.7
14a	423	4	2.20	1.24	102.82	7.27 ± 0.09[d]	42.8
14b	451	4	2.91	1.94	102.82	7.34 ± 0.03[d]	46.8
14d	395	6	1.44	0.50	124.82	7.43 ± 0.10[d]	51.8
II	378	7	1.73	−1.25	113.97	10.34 ± 0.04[d]	99.9
15a	438	5	2.25	1.26	114.85	7.95 ± 0.05[d]	78.2
15b	466	5	2.97	1.96	114.85	8.27 ± 0.07[d]	88.2
15d	410	7	1.50	0.52	136.85	ND[e]	ND
15e	590	5	5.70	4.68	114.85	ND	ND
III	348	5	3.12	−0.27	72.84	10.71 ± 0.10[d]	99.95
16a	408	3	3.64	2.55	73.72	8.01 ± 0.12[d]	80.4
16b	436	3	4.36	3.23	73.72	8.01 ± 0.21[d]	80.4
16d	380	5	2.89	1.83	95.72	7.97 ± 0.13[d]	78.7
IV	346	5	2.79	−060	72.84	9.82 ± 0.26	99.6
17a	406	3	3.32	2.22	73.72	7.53 ± 0.14	57.4
17d	378	5	2.56	1.50	95.72	ND	ND
V	332	5	2.35	−1.09	72.84	10.12 ± 0.17	99.8

[a] The molecular weight, clog*P* values, polar surface area (PSA), and log$D_{7.4}$ were calculated using the ChemAxon software MarvinSketch v.5.11.1.
[b] Calculated with the weighted method considering tautomerization/resonance and an electrolyte concentration of 0.1 mol/dm^3 and using a training set containing the experimental pK_a values of 21 related compounds.
[c] Measured by UV spectrophotometry in H_2O-DMSO (2%, vol/vol) at 30°C as described previously (25). Values are the means from 3 independent determinations ± SD. Only one pK_a could be calculated for both imidazoline rings in the molecule.
[d] Taken from reference 25.
[e] ND, not determined due to solubility problems in the buffers used for pK_a determination.

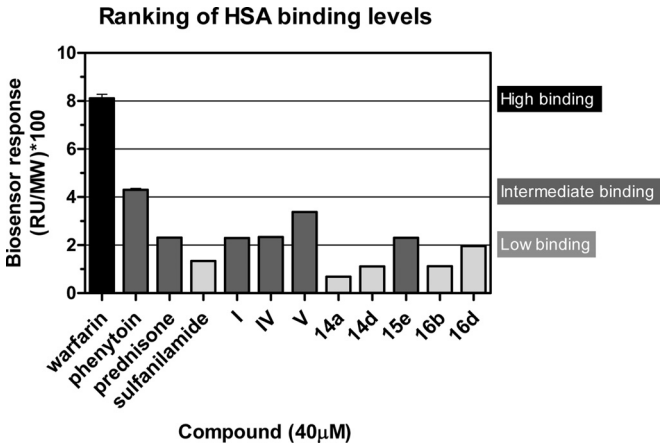

FIG 3 Plot of HSA binding levels determined by SPR for the lead compounds (I, IV, and V) and the *N*-alkoxy (14a, 15e, and 16b) and *N*-hydroxy (14d and 16d) derivatives. The compounds were ranked as high-level HSA binders (black), intermediate binders (deep gray), and low binders (pale gray) based on the binding affinity of the four control drugs warfarin, phenytoin, prednisone, and sulfanilamide. MW, molecular weight.

HSA were used as controls: warfarin, phenytoin, prednisone, and sulfanilamide. This allowed the classification of the compounds into regions of high, intermediate, and low binding to HSA (Fig. 3). All of the compounds tested showed reversible binding to HSA. A representative set of compounds (i.e., lead compounds and *N*-OH, *N*-OMe, *N*-OEt, and *N*-OBn derivatives), including the most interesting one (14d), was assayed. The dicationic lead compounds (I, IV, and V) and analogue 15e exhibited intermediate binding (in the range of prednisone and phenytoin), whereas *N*-alkoxy (14a and 16b) and *N*-hydroxy (14d and 16d) derivatives displayed low binding to HSA. This low binding level to plasma proteins is expected to positively influence the antiparasitic activity of these compounds by increasing their free concentration in the blood.

***In vitro* study of hepatic metabolism by amidoxime reductases.** Since the most active compound (14d) in the late-stage disease is an *N*-hydroxy imidazoline derivative that is structurally related to *N*-hydroxyguanidines and amidoximes, we investigated whether this compound could be reduced to parent compound I by amidoxime reductases under the same conditions as those described for amidoxime (e.g., benzamidoxime and *N*-hydroxypentamidine) and *N*-hydroxyguanidine prodrugs (e.g., guanoxabenz and *N*-hydroxydebrisoquine) (39–41). This is important, because if 14d is metabolized by amidoxime reductases, it may work as a prodrug of compound I.

Incubations of 14d with human liver microsomes or human liver mitochondria in the presence of NADH as a cofactor were carried out in two different buffers (pH 6 and 7.4) for 60 min. No reduction of 14d was observed by reverse-phase (RP)-HPLC compared with the corresponding controls analyzed under the same conditions but without enzymatic fractions (see the chromatogram in Fig. S2 in the supplemental material). The absence of a reduction of 14d to the double *N*-dehydroxylated compound I under the conditions investigated was confirmed by HPLC-MS. No intermediate metabolites corresponding to a single *N*-dehydroxylation were observed under those incubations compared with controls. In contrast, benzamidoxime, which is commonly used as a reference substrate of *N*-hydroxylamine or amidoxime reductases, was reduced to benzamidine by the same hepatic subcellular fractions. The metabolic rate obtained for the formation of benzamidine from benzamidoxime was 0.86 and 0.26 nmol/min/mg of protein for human liver microsomes and human liver mitochondria, respectively (details of these experiments can be found in the supplemental material). Therefore, we conclude that 14d does not work as a prodrug of I, and its efficacy against *T. brucei* most probably is due to its intrinsic activity against the parasite (IC_{50}, 0.89 μM; SI, >240).

***In vitro* determination of compound permeability across the blood-brain barrier.** The capacity of compounds 14d and V (which showed significant activity in the mouse model of CNS infection) to cross the BBB was measured *in vitro* using the immortalized human brain endothelial cell line hCMEC/D3 (42), which has proved useful as an *in vitro* BBB model (43). This cellular model is able to discriminate between compounds with low, medium, and high permeability across the BBB. The permeability of the reference drug pentamidine, which is known to have low CNS bioavailability and does not cure late-stage HAT (44), I, and III also were measured as a means of comparison.

In order to measure distribution across an hCMEC/D3 layer, cells were cultured in a Boyden chamber-like system, with the luminal and abluminal compartments representing the blood and cerebral compartments, respectively (32). Test compounds were loaded in the luminal compartment, and after a preset time, their amounts in both compartments were determined by HPLC, yielding the mass balance. The clearance principle (i.e., the slope of the volume of drug cleared from the luminal compartment to the abluminal one versus time) was used to calculate the permeability coefficients (23, 45). The small hydrophilic compound Lucifer yellow (LY), the diffusion of which is strongly restricted at the BBB level, was used as a marker of paracellular permeation and as a control for low permeability. LY permeability ($1.63 \times 10^{-3} \pm 0.09 \times 10^{-3}$ cm/min) was attributed the value of 100%; pentamidine permeability was very similar (91% versus 100%; see Fig. S3a in the supplemental material).

The lead compounds I, III, and V all displayed similar permeability values (133%, 142%, and 138%, respectively; see Fig. S3a in the supplemental material). Although slightly higher than that of LY, these values represent a low BBB permeability in this model compared to those of phenytoin (5.62×10^{-3} cm/min; 345%) and diazepam (120×10^{-3} cm/min; 7,362%), which are used as markers for medium and high BBB permeability, respectively (46). The permeability value of 14d was significantly lower than that of lead compound I in this assay. The possible metabolism of the compounds by hCMEC/D3 cells was disregarded, as the mass balance for all of the compounds was ~100% in all of the experiments.

To check whether our assay was able to detect the passage of 14d despite its low permeability, the endothelial layer was hyperosmotically challenged with a 1.4 M solution of mannitol, temporarily disrupting tight junctions and allowing free paracellular diffusion. Hyperosmotic shock robustly increased LY and 14d permeabilities (692% versus 100% for LY alone and 217% versus 49% for 14d alone; see Fig. S3b in the supplemental material). However, 14d may reach the brain by different routes than the paracellular pathway or free diffusion across both endothelial plasma membranes (e.g., transcytosis or active transport) (47). BSA was added to the buffer in order to increase any transcytosis of 14d; however, it reduced permeability for this compound, if anything (28% compared to 49% for 14d alone; see Fig. S3b).

DISCUSSION

New *N*-alkoxy and *N*-hydroxy derivatives of bisimidazoline lead compounds were synthesized to reduce their polarity and potentially improve their *in vivo* antitrypanosomal activity against late-stage sleeping sickness. To treat this stage of the disease, which is characterized by the presence of trypanosomes in the brain and cerebrospinal fluid, drugs with the ability to cross the BBB are required. Since bisimidazolines are dicationic molecules at physiological pH, their BBB permeability may be compromised, as previously observed with other dicationic compounds. In the case of the diamidine drugs pentamidine and furamidine, which are carried into the brain through influx transporters, limited CNS availability is the result of the concomitant sequestration within the capillary endothelium and rapid efflux by P-glycoproteins (44, 48). In the present study, we have shown that *N*-OR-substituted imidazoline derivatives have lower pK_a values than their unsubstituted analogues (approximately 2 pK_a units); therefore, they are less ionized at physiological pH. Compound 14d, which is only 50% ionized at pH 7.4, was the most active compound of the series, being curative in the hemolymphatic stage and weakly active against the CNS stage of the infection in mice. In contrast, derivative 14b, which has a pK_a value similar to that of 14d, was inactive (data not shown), probably due to its low *in vitro* activity against the parasite. Alternatively, this may be the result of different interactions with the putative diamidine transporters and/or P-glycoprotein efflux pumps expressed at the BBB (44).

Compound 14d showed similar susceptibilities toward wild-type and drug-resistant strains of trypanosomes lacking the *Tb*AT1/P2 aminopurine transporter and the HAPT transporter (TbAT1-KO and B48, respectively). This indicates that these transporters are not essential for the uptake of this compound *in vitro*. Hence, 14d should not be prone to cross-resistance with other trypanocidal drugs, such as diamidines and arsenicals (31).

The more active antitrypanosomal compounds in the chronic model of HAT (14d and V) presented a low *in vitro* permeability value in the hCMEC/D3 model of BBB. However, the differential expression of transporters and metabolizing enzymes at the BBB is one of the main factors that significantly contribute to the interindividual variation in the bioavailability and vulnerability to drugs and xenobiotics (49, 50). Hence, species differences could account for the divergences observed between *in vitro* BBB permeability assays with human cells and *in vivo* results in murine models of HAT. It is possible that, in contrast to the passive diffusion hypothesis, brain uptake of 14d happens mainly through a specific transporter that is expressed in mice but not in the human hCMEC/D3 cell line (51). In fact, slight differences regarding ABC transporter expression have been observed between this cell line and microvessels isolated from human brain (52). Moreover, the dicationic diamidine DB829 is curative in the same murine model of late-stage trypanosomiasis, although its close analogues DB75 and diminazene have no activity at all against the cerebral infection (53). This is clear proof that highly specific transporters for diamidine analogues exist on the murine BBB, with sufficient capacity to facilitate the entry of curative levels of such compounds into the brain (54). Moreover, the fact that 14d hardly binds to plasma proteins (<20%) gives rise to a higher free plasma concentration of the compound, which in turn makes it more available to such solute transporters and leads to higher activity *in vivo* in the mouse model of stage 2 sleeping sickness.

Altogether, these data show that the hydroxy derivative 14d is more effective in the CNS stage of HAT than the unsubstituted lead compound I, and it has a larger therapeutic index *in vivo* in mice. Apparently, 14d is able to reach the brain in a specific manner, across an intact BBB, but it does not cross the BBB in sufficient amounts to cure the CNS infection with the dosage/administration scheme used in this study. Further investigations to elucidate the nature of the transporter(s) involved will be needed, as well as a complete pharmacokinetic analysis to determine the levels of 14d in the mouse brain.

The observations with 14d appear similar to those with the *N*-methoxyamidine prodrug pafuramidine (DB289), which, in contrast to the active diamidine DB75, penetrates the BBB unaltered and is subject to biotransformation within the brain (48). However, unlike DB289, cerebral uptake of 14d is not believed to be the result of simple diffusion across the BBB, and we have further shown here that 14d was not metabolized *in vitro* by amidoxime reductases that are present in human hepatic microsomal and mitochondrial fractions. Hence, 14d is likely to be the active molecule that inhibits trypanosome growth within the brain.

Among the new compounds reported here, the *N*-hydroxy derivatives 14d to 17d have shown better activity/selectivity profiles *in vitro* and higher activity *in vivo* than other *N*-alkoxy derivatives. On the one hand, these results confirm previous findings on similar series of *N*-hydroxy imidazolines (8). On the other hand, this is different from a series of diamidoxime (i.e., di-*N*-hydroxy amidines) metabolites, which were found to be less active *in vivo* than the monoamidoxime/monomethoxyamidine metabolites of the dimethoxyamidine prodrugs (53).

Regarding the mode of action of the antitrypanosomal lead compounds I to V, earlier studies have shown that this class of dicationic compounds binds to the DNA minor groove at AT-rich sequences (55–58). In trypanosomes, the kinetoplast DNA (kDNA) has a high content of AT-rich regions that could be a site of selective action of this kind of compound (59). In fact, some correlation between DNA binding and *in vitro* antitrypanosomal activity was observed, suggesting a mode of action due in part to the formation of a DNA complex (9). Interestingly, we have observed that the *N*-alkoxy (14a to c, 15a to c, and 16a to c) and *N*-hydroxy derivatives (14d, 15d, and 16d) also bind selectively to AT-rich DNA, some of them, such as 14d, with affinity in the same range as that of the unsubstituted, dicationic lead compound (C. H. Ríos Martínez and C. Dardonville, unpublished data). Further work to elucidate the interaction of these compounds with DNA will be the subject of a different paper.

Conclusions. We have shown here that introducing alkoxy and hydroxy substituents (OR; R = H, Me, Et) at position N1 of the imidazoline rings reduces the basicity of aminoimidazoline compounds by approximately 2 pK_a units. While the nature of the R substituent does not significantly alter the pK_a in a homologous series ($\Delta pK_a \leq 0.2$ for R = H ≈ Me ≈ Et), its impact on *in vivo* activity is significant. The *N*-hydroxy-substituted compound showed efficacy in models of first- and second-stage *T. brucei* infection in mice, whereas *N*-OMe and *N*-OEt analogues did not. In addition, *N*-hydroxy derivatives were less cytotoxic and better tolerated *in vivo*. The activity profile demonstrated by 14d *in vitro* and *in vivo* in both experimental models of HAT, and the absence of hepatic metabolism observed *in vitro* (i.e., N-OH reduction by amidoxime reductases), indicate that 14d, and possibly other *N*-hydroxy imidazoline derivatives, represents a new class of prom-

ising antitrypanosomal agents. This class of compounds appears to have activity against *T. brucei*, a favorable drug resistance profile, more favorable physicochemical properties (e.g., lower pK_a and low level of protein binding), and a higher therapeutic index than the unsubstituted parent compounds, indicating good progress toward the discovery of new drugs for late-stage sleeping sickness. Hence, further optimization of these compounds in an effort to obtain CNS-curative trypanocidal agents is warranted.

Finally, it is noteworthy that the bisimidazolinium fluorene lead compound V was curative in the STIB900 mouse model for acute African trypanosomiasis, whereas its guanidine analogue was inactive *in vivo* (60). This finding illustrates once again the superiority of the (4,5-dihydro-1*H*-imidazol-2-yl)amino group over guanidine as a useful cationic moiety for the design of antitrypanosomal compounds.

ACKNOWLEDGMENTS

This work was supported by grants from the Spanish Ministerio de Ciencia e Innovación (grant SAF2009-10399) and the CSIC (bilateral project grants 2008GB0021 and PA1003015) to C.D. and a CSIC grant (project 200470E658) to T.H. C.R. was the recipient of a Ph.D. fellowship from the government of Panama (SENACYT grant BIDP-2008-030). This work was awarded the GlaxoSmithKline prize from the Spanish Society of Medicinal Chemistry to C.R. (XV Convocatoria de Premios para Investigadores Noveles en el Campo de la Búsqueda y Desarrollo de Nuevos Fármacos). A.A.E. was supported by a British Commonwealth Scholarship.

We thank Pierre-Olivier Couraud for logistical collaboration. The contributions of Elsa Berthaut to pK_a measurements and Eddysson Jamir Flores Pérez to the synthesis of 15a and 16b are gratefully acknowledged.

REFERENCES

1. **WHO.** 2010. Working to overcome the global impact of neglected tropical diseases: first WHO report on neglected tropical diseases. World Health Organization, Geneva, Switzerland.
2. **Rodgers J.** 2009. Human African trypanosomiasis, chemotherapy and CNS disease. J Neuroimmunol **211:**16–22. http://dx.doi.org/10.1016/j.jneuroim.2009.02.007.
3. **Steverding D.** 2010. The development of drugs for treatment of sleeping sickness: a historical review. Parasites Vectors **3:**15. http://dx.doi.org/10.1186/1756-3305-3-15.
4. **Soeiro MNC, De Souza EM, Stephens CE, Boykin DW.** 2005. Aromatic diamidines as antiparasitic agents. Expert Opin Investig Drugs **14:**957–972. http://dx.doi.org/10.1517/13543784.14.8.957.
5. **Paine MF, Wang MZ, Generaux CN, Boykin DW, Wilson WD, De Koning HP, Olson CA, Pohlig G, Burri C, Brun R, Murilla GA, Thuita JK, Barrett MP, Tidwell RR.** 2010. Diamidines for human African trypanosomiasis. Curr Opin Investig Drugs **11:**876–883.
6. **Dardonville C, Barrett MP, Brun R, Kaiser M, Tanious F, Wilson WD.** 2006. DNA binding affinity of bisguanidine and bis(2-aminoimidazoline) derivatives with in vivo antitrypanosomal activity. J Med Chem **49:**3748–3752. http://dx.doi.org/10.1021/jm060295c.
7. **Dardonville C, Brun R.** 2004. Bisguanidine, bis(2-aminoimidazoline), and polyamine derivatives as potent and selective chemotherapeutic agents against *Trypanosoma brucei rhodesiense*. Synthesis and in vitro evaluation. J Med Chem **47:**2296–2307. http://dx.doi.org/10.1021/jm031024u.
8. **Nieto L, Mascaraque A, Miller F, Glacial F, Ríos Martínez C, Kaiser M, Brun R, Dardonville C.** 2011. Synthesis and antiprotozoal activity of N-alkoxy analogues of the trypanocidal lead compound 4,4′-bis(imidazolinylamino)diphenylamine with improved human blood-brain barrier permeability. J Med Chem **54:**485–494. http://dx.doi.org/10.1021/jm101335q.
9. **Rodríguez F, Rozas I, Kaiser M, Brun R, Nguyen B, Wilson WD, García RN, Dardonville C.** 2008. New bis(2-aminoimidazoline) and bisguanidine DNA minor groove binders with potent in vivo antitrypanosomal and antiplasmodial activity. J Med Chem **51:**909–923. http://dx.doi.org/10.1021/jm7013088.
10. **Takimiya K, Yanagimoto T, Yamashiro T, Ogura F, Otsubo T.** 1998. Syntheses and properties of 11,11,12,12-tetracyano-2,6-anthraquinodimethane (TANT) and its 9,10-dichloro derivative as novel extensive electron acceptors. Bull Chem Soc Jpn **71:**1431–1435. http://dx.doi.org/10.1246/bcsj.71.1431.
11. **Räz B, Iten M, Grether-Bühler Y, Kaminsky R, Brun R.** 1997. The Alamar Blue assay to determine drug sensitivity of African trypanosomes (*T. b. rhodesiense* and *T. b. gambiense*) in vitro. Acta Trop **68:**139–147. http://dx.doi.org/10.1016/S0001-706X(97)00079-X.
12. **O'Brien J, Wilson I, Orton T, Pognan F.** 2000. Investigation of the Alamar Blue (resazurin) fluorescent dye for the assessment of mammalian cell cytotoxicity. Eur J Biochem **267:**5421–5426. http://dx.doi.org/10.1046/j.1432-1327.2000.01606.x.
13. **Dardonville C, Fernandez-Fernandez C, Gibbons SL, Jagerovic N, Nieto L, Ryan G, Kaiser M, Brun R.** 2009. Antiprotozoal activity of 1-phenethyl-4-aminopiperidine derivatives. Antimicrob Agents Chemother **53:**3815–3821. http://dx.doi.org/10.1128/AAC.00124-09.
14. **Rodenko B, Van Der Burg AM, Wanner MJ, Kaiser M, Brun R, Gould M, De Koning HP, Koomen GJ.** 2007. 2,N6-disubstituted adenosine analogs with antitrypanosomal and antimalarial activities. Antimicrob Agents Chemother **51:**3796–3802. http://dx.doi.org/10.1128/AAC.00425-07.
15. **Matovu E, Stewart ML, Geiser F, Brun R, Maser P, Wallace LJM, Burchmore RJ, Enyaru JCK, Barrett MP, Kaminsky R, Seebeck T, De Koning HP.** 2003. Mechanisms of arsenical and diamidine uptake and resistance in Trypanosoma brucei. Eukaryot Cell **2:**1003–1008. http://dx.doi.org/10.1128/EC.2.5.1003-1008.2003.
16. **Bridges DJ, Gould MK, Nerima B, Maser P, Burchmore RJS, De Koning HP.** 2007. Loss of the high-affinity pentamidine transporter is responsible for high levels of cross-resistance between arsenical and diamidine drugs in African trypanosomes. Mol Pharmacol **71:**1098–1108. http://dx.doi.org/10.1124/mol.106.031351.
17. **Thuita JK, Karanja SM, Wenzler T, Mdachi RE, Ngotho JM, Kagira JM, Tidwell R, Brun R.** 2008. Efficacy of the diamidine DB75 and its prodrug DB289, against murine models of human African trypanosomiasis. Acta Trop **108:**6–10. http://dx.doi.org/10.1016/j.actatropica.2008.07.006.
18. **Baltz T, Baltz D, Giroud C, Crockett J.** 1985. Cultivation in a semi-defined medium of animal infective forms of *Trypanosoma brucei*, *T. equiperdum*, *T. evansi*, *T. rhodesiense*, and *T. gambiense* EMBO J **4:**1273–1277.
19. **Desjardins RE, Canfield CJ, Haynes JD, Chulay JD.** 1979. Quantitative assessment of antimalarial activity in vitro by a semiautomated microdilution technique. Antimicrob Agents Chemother **16:**710–718. http://dx.doi.org/10.1128/AAC.16.6.710.
20. **Thaithong S, Beale GH, Chutmongkonkul M.** 1983. Susceptibility of Plasmodium falciparum to five drugs: an in vitro study of isolates mainly from Thailand. Trans R Soc Trop Med Hyg **77:**228–231. http://dx.doi.org/10.1016/0035-9203(83)90080-9.
21. **Buckner FS, Verlinde CL, La Flamme AC, Van Voorhis WC.** 1996. Efficient technique for screening drugs for activity against Trypanosoma cruzi using parasites expressing beta-galactosidase. Antimicrob Agents Chemother **40:**2592–2597.
22. **Jennings FW, Gray GD.** 1983. Relapsed parasitaemia following chemotherapy of chronic T. brucei infections in mice and its relation to cerebral trypanosomes. Contrib Microbiol Immunol **7:**147–154.
23. **Siflinger-Birnboim A, del Vecchio PJ, Cooper JA, Blumenstock FA, Shepard JM, Malik AB.** 1987. Molecular sieving characteristics of the cultured endothelial monolayer. J Cell Physiol **132:**111–117. http://dx.doi.org/10.1002/jcp.1041320115.
24. **Cecchelli R, Dehouck B, Descamps L, Fenart L, Buée-Scherrer V, Duhem C, Lundquist S, Rentfel M, Torpier G, Dehouck MP.** 1999. In vitro model for evaluating drug transport across the blood-brain barrier. Adv Drug Deliv Rev **36:**165–178. http://dx.doi.org/10.1016/S0169-409X(98)00083-0.
25. **Ríos Martínez CH, Dardonville C.** 2013. Rapid determination of ionization constants (pK_a) by UV spectroscopy using 96-well microtiter plates. ACS Med Chem Lett **4:**142–145. http://dx.doi.org/10.1021/ml300326v.
26. **Rodriguez F, Rozas I, Ortega JE, Erdozain AM, Meana JJ, Callado LF.** 2008. Guanidine and 2-aminoimidazoline aromatic derivatives as α2-adrenoceptor antagonists. 2. Exploring alkyl linkers for new antidepressants. J Med Chem **51:**3304–3312. http://dx.doi.org/10.1021/jm800026x.
27. **Mascaraque A, Nieto L, Dardonville C.** 2008. Efficient one-pot synthesis of 1-alkoxy-2-arylaminoimidazolines from N-alkoxy-N-(2-aminoethyl)-

2-nitrobenzenesulfonamides and arylisothiocyanates. Tetrahedron Lett **49:**4571–4574. http://dx.doi.org/10.1016/j.tetlet.2008.05.098.
28. **Fu PP, Harvey RG.** 1978. Dehydrogenation of polycyclic hydroaromatic compounds. Chem Rev **78:**317–361. http://dx.doi.org/10.1021/cr60314a001.
29. **De Koning HP, Jarvis SM.** 2001. Uptake of pentamidine in Trypanosoma brucei brucei is mediated by the P2 adenosine transporter and at least one novel, unrelated transporter. Acta Trop **80:**245–250. http://dx.doi.org/10.1016/S0001-706X(01)00177-2.
30. **De Koning HP.** 2001. Uptake of pentamidine in Trypanosoma brucei bruceiis mediated by three distinct transporters: implications for cross-resistance with arsenicals. Mol Pharmacol **59:**586–592. http://dx.doi.org/10.1124/mol.59.3.586.
31. **De Koning HP.** 2008. Ever-increasing complexities of diamidine and arsenical crossresistance in African trypanosomes. Trends Parasitol **24:**345–349. http://dx.doi.org/10.1016/j.pt.2008.04.006.
32. **De Koning HP, Jarvis SM.** 1999. Adenosine transporters in bloodstream forms of Trypanosoma brucei brucei: substrate recognition motifs and affinity for trypanocidal drugs. Mol Pharmacol **56:**1162–1170.
33. **Torreele E, Bourdin Trunz B, Tweats D, Kaiser M, Brun R, Mazué G, Bray MA, Pécoul B.** 2010. Fexinidazole: a new oral nitroimidazole drug candidate entering clinical development for the treatment of sleeping sickness. PLoS Negl Trop Dis **4:**e923. http://dx.doi.org/10.1371/journal.pntd.0000923.
34. **Ghuman J, Zunszain PA, Petitpas I, Bhattacharya AA, Otagiri M, Curry S.** 2005. Structural basis of the drug-binding specificity of human serum albumin. J Mol Biol **353:**38–52. http://dx.doi.org/10.1016/j.jmb.2005.07.075.
35. **Bertucci C, Domenici E.** 2002. Reversible and covalent binding of drugs to human serum albumin: methodological approaches and physiological relevance. Curr Med Chem **9:**1463–1481. http://dx.doi.org/10.2174/0929867023369673.
36. **Craig WA, Ebert SC.** 1989. Protein binding and its significance in antibacterial therapy. Infect Dis Clin North Am **3:**407–414.
37. **Frostell-Karlsson Å, Remaeus A, Roos H, Andersson K, Borg P, Hämäläinen M, Karlsson R.** 2000. Biosensor analysis of the interaction between immobilized human serum albumin and drug compounds for prediction of human serum albumin binding levels. J Med Chem **43:**1986–1992. http://dx.doi.org/10.1021/jm991174y.
38. **Rich RL, Day YSN, Morton TA, Myszka DG.** 2001. High-resolution and high-throughput protocols for measuring drug/human serum albumin interactions using BIACORE. Anal Biochem **296:**197–207. http://dx.doi.org/10.1006/abio.2001.5314.
39. **Gruenewald S, Wahl B, Bittner F, Hungeling H, Kanzow S, Kotthaus J, Schwering U, Mendel RR, Clement B.** 2008. The fourth molybdenum containing enzyme mARC: cloning and involvement in the activation of N-hydroxylated prodrugs. J Med Chem **51:**8173–8177. http://dx.doi.org/10.1021/jm8010417.
40. **Clement B, Mau S, Deters S, Havemeyer A.** 2005. Hepatic, extrahepatic, microsomal, and mitochondrial activation of the N-hydroxylated prodrugs benzamidoxime, guanoxabenz, and Ro 48-3656 ([[1-[(2s)-2-[[4-[(hydroxyamino)iminomethyl]benzoyl]amino]-1-oxopropyl]-4-piperidinyl]oxy]-acetic acid). Drug Metab Dispos **33:**1740–1747. http://dx.doi.org/10.1124/dmd.105.005249.
41. **Boykin DW, Kumar A, Hall JE, Bender BC, Tidwell RR.** 1996. Antipneumocystis activity of bis-amidoximes and bis-O-alkylamidoximes prodrugs. Bioorg Med Chem Lett **6:**3017–3020. http://dx.doi.org/10.1016/S0960-894X(96)00557-4.
42. **Weksler BB, Subileau EA, Perriere N, Charneau P, Holloway K, Leveque M, Tricoire-Leignel H, Nicotra A, Bourdoulous S, Turowski P, Male DK, Roux F, Greenwood J, Romero IA, Couraud PO.** 2005. Blood-brain barrier-specific properties of a human adult brain endothelial cell line. FASEB J **19:**1872–1874. http://dx.doi.org/10.1096/fj.04-3458fje.
43. **Poller B, Gutmann H, Krähenbühl S, Weksler B, Romero I, Couraud P-O, Tuffin G, Drewe J, Huwyler J.** 2008. The human brain endothelial cell line hCMEC/D3 as a human blood-brain barrier model for drug transport studies. J Neurochem **107:**1358–1368. http://dx.doi.org/10.1111/j.1471-4159.2008.05730.x.
44. **Sanderson L, Dogruel M, Rodgers J, De Koning HP, Thomas SA.** 2009. Pentamidine movement across the murine blood-brain and blood-cerebrospinal fluid barriers: effect of trypanosome infection, combination therapy, P-glycoprotein, and multidrug resistance-associated protein. J Pharmacol Exp Ther **329:**967–977. http://dx.doi.org/10.1124/jpet.108.149872.
45. **Deli MA, Abrahám C, Kataoka Y, Niwa M.** 2005. Permeability studies on in vitro blood-brain barrier models: physiology, pathology, and pharmacology. Cell Mol Neurobiol **25:**59–127. http://dx.doi.org/10.1007/s10571-004-1377-8.
46. **Cucullo L, Couraud PO, Weksler B, Romero IA, Hossain M, Rapp E, Janigro D.** 2008. Immortalized human brain endothelial cells and flow-based vascular modeling: a marriage of convenience for rational neurovascular studies. J Cereb Blood Flow Metab **28:**312–328. http://dx.doi.org/10.1038/sj.jcbfm.9600525.
47. **Scherrmann J-M.** 2009. Transporters in absorption, distribution, and elimination. Chem Biodivers **6:**1933–1942. http://dx.doi.org/10.1002/cbdv.200900171.
48. **Sturk LM, Brock JL, Bagnell CR, Hall JE, Tidwell RR.** 2004. Distribution and quantitation of the anti-trypanosomal diamidine 2,5-bis(4-amidinophenyl)furan (DB75) and its N-methoxy prodrug DB289 in murine brain tissue. Acta Trop **91:**131–143. http://dx.doi.org/10.1016/j.actatropica.2004.03.010.
49. **Ronaldson PT, Babakhanian K, Bendayan R.** 2006. Drug transport in the brain. John Wiley & Sons, Inc, New York, NY.
50. **Klaassen CD, Cheng X.** 2006. Age- and gender-related differences in xenobiotic transporter expression. John Wiley & Sons, Inc, New York, NY.
51. **Ohtsuki S, Ikeda C, Uchida Y, Sakamoto Y, Miller F, Glacial F, Decleves X, Scherrmann J-M, Couraud P-O, Kubo Y, Tachikawa M, Terasaki T.** 2013. Quantitative targeted absolute proteomic analysis of transporters, receptors and junction proteins for validation of human cerebral microvascular endothelial cell line hCMEC/D3 as a human blood-brain barrier model. Mol Pharm **10:**289–296. http://dx.doi.org/10.1021/mp3004308.
52. **Dauchy S, Miller F, Couraud PO, Weaver RJ, Weksler B, Romero IA, Scherrmann JM, De Waziers I, Decleves X.** 2009. Expression and transcriptional regulation of ABC transporters and cytochromes P450 in hCMEC/D3 human cerebral microvascular endothelial cells. Biochem Pharmacol **77:**897–909. http://dx.doi.org/10.1016/j.bcp.2008.11.001.
53. **Wenzler T, Boykin DW, Ismail MA, Hall JE, Tidwell RR, Brun R.** 2009. New treatment option for second-stage African sleeping sickness: in vitro and in vivo efficacy of Aza analogs of DB289. Antimicrob Agents Chemother **53:**4185–4192. http://dx.doi.org/10.1128/AAC.00225-09.
54. **Yang S, Wenzler T, Miller PN, Wu H, Boykin DW, Brun R, Wang MZ.** 2014. Pharmacokinetic comparison to determine the mechanisms underlying the differential efficacies of cationic diamidines against first- and second-stage human African trypanosomiasis. Antimicrob Agents Chemother **58:**4064–4074. http://dx.doi.org/10.1128/AAC.02605-14.
55. **Glass LS, Nguyen B, Goodwin KD, Dardonville C, Wilson WD, Long EC, Georgiadis MM.** 2009. Crystal structure of a trypanocidal 4,4′-bis(imidazolinylamino)diphenylamine bound to DNA. Biochemistry **48:**5943–5952. http://dx.doi.org/10.1021/bi900204w.
56. **Nagle PS, Rodriguez F, Nguyen B, Wilson WD, Rozas I.** 2012. High DNA affinity of a series of peptide linked diaromatic guanidinium-like derivatives. J Med Chem **55:**4397–4406. http://dx.doi.org/10.1021/jm300296f.
57. **Nagle PS, Quinn SJ, Kelly JM, O'Donovan DH, Khan AR, Rodriguez F, Nguyen B, Wilson WD, Rozas I.** 2010. Understanding the DNA binding of novel non-symmetrical guanidinium/2-aminoimidazolinium derivatives. Org Biomol Chem **8:**5558–5567. http://dx.doi.org/10.1039/c0ob00428f.
58. **Ríos Martínez CH, Lagartera L, Kaiser M, Dardonville C.** 2014. Antiprotozoal activity and DNA binding of N-substituted N-phenylbenzamide and 1,3-diphenylurea bisguanidines. Eur J Med Chem **81:**481–491. http://dx.doi.org/10.1016/j.ejmech.2014.04.083.
59. **Wilson WD, Nguyen B, Tanious FA, Mathis A, Hall JE, Stephens CE, Boykin DW.** 2005. Dications that target the DNA minor groove: compound design and preparation, DNA interactions, cellular distribution and biological activity. Curr Med Chem Anticancer Agents **5:**389–408. http://dx.doi.org/10.2174/1568011054222319.
60. **Arafa RK, Brun R, Wenzler T, Tanious FA, Wilson WD, Stephens CE, Boykin DW.** 2005. Synthesis, DNA affinity, and antiprotozoal activity of fused ring dicationic compounds and their prodrugs. J Med Chem **48:**5480–5488. http://dx.doi.org/10.1021/jm058190h.
61. **Patrick DA, Bakunov SA, Bakunova SM, Jones SK, Wenzler T, Barszcz T, Kumar A, Boykin DW, Werbovetz KA, Brun R, Tidwell RR.** 2013. Synthesis and antiprotozoal activities of benzyl phenyl ether diamidine derivatives. Eur J Med Chem **67:**310–324. http://dx.doi.org/10.1016/j.ejmech.2013.06.033.